Distribution Agreement

In presenting this thesis or dissertation as a partial fulfillment of the requirements for an advanced degree from Emory University, I hereby grant to Emory University and its agents the non-exclusive license to archive, make accessible, and display my thesis or dissertation in whole or in part in all forms of media, now or hereafter known, including display on the world wide web. I understand that I may select some access restrictions as part of the online submission of this thesis or dissertation. I retain all ownership rights to the copyright of the thesis or dissertation. I also retain the right to use in future works (such as articles or books) all or part of this thesis or dissertation.

Signature:

_____ _____

Yuanyuan Fang Date

Quantification of Microvessel Density in Hepatocellular Carcinoma with Whole-slide Digital Analysis – Its Clinical and Prognostic Significance, and Associations with PDGFR-α, PDGFR-β, and VEGFR2

By

Yuanyuan Fang

Master of Public Health

Epidemiology

_____

Roberd Bostick

Faculty Thesis Advisor

_____

Alton Farris

Thesis Field Advisor

Quantification of Microvessel Density in Hepatocellular Carcinoma with Whole-slide Digital Analysis – Its Clinical and Prognostic Significance, and Associations with PDGFR-α, PDGFR-β, and VEGFR2

By

Yuanyuan Fang

Master of Medicine, Nankai University, 2010

Bachelor of Medicine, Nankai University, 2008

Faculty Thesis Advisor: Roberd Bostick, MD, MPH

An abstract of

A thesis submitted to the Faculty of the

Rollins School of Public Health of Emory University

In partial fulfillment of the requirements for the degree of

Master of Public Health

In Epidemiology

2012

Abstract

Quantification of Microvessel Density in Hepatocellular Carcinoma with Whole-slide Digital Aanalysis – Its Clinical and Prognostic Significance, and Associations with PDGFR-α, PDGFR-β, and VEGFR2

By Yuanyuan Fang

Aims: To investigate the following correlations/associations related to evaluations of whole-slide digital analysis of tumors in patients undergoing resections of hepatocellular carcinoma (HCC): 1) between two different methods of microvessel density (MVD) evaluation, developed by Weiss et al and Tanigawa et al, respectively; 2) between whole slide digital analysis and manual grading of expression of platelet derived growth factor receptor-α (PDGFR-α), platelet derived growth factor receptor-β (PDGFR-β), and vascular endothelial growth factor receptor 2 (VEGFR2); 3) of tumor MVD with clinicopathologic characteristics and postoperative overall survival; and 4) of PDGFR-α, PDGFR-β, and VEGFR2 expression with MVD, clinicopathologic characteristics, and postoperative overall survival.

Methods: Tumor MVD was assessed in 47 patients with resected HCC using the Aperio microvessel analysis algorithm after immunostaining for CD31. Expression of PDGFR-α, PDGFR-β, and VEGFR2 in HCCs was assessed using the Aperio positive pixel count algorithm. Patients were prospectively followed until their death.

Results: 1) We observed a good agreement between the two MVD evaluation methods (r=0.95; kappa=0.87). 2) The average intensity (the inverse of the optical density) of the biomarker staining was most highly correlated with manual grading (r=0.69 for PDGFR-α; r=0.69 for PDGFR-β; and r=0.82 for VEGFR2). 3) Higher MVD was statistically significantly associated with a negative microscopic margin (p=0.004) and a smaller tumor size (≤5cm) (p=0.003). A higher MVD and a lower PDGFR-α expression together were the most strongly associated with a better overall survival (HR: 0.014; 95% CI: 0.001,0.23) among female patients without microvascular invasion of HCCs. 4) We found no significant associations of PDGFR-α , PDGFR-β, and VEGFR2, or MVD with the clinicopathologic characteristics.

Conclusion: There was a good agreement between the two MVD assessing methods. Higher MVD was found in small HCCs (<5cm) and HCCs with a negative microscopic margin. MVD together with PDGFR-α may be useful as a prognostic marker combination among female patients with microvascular invasion of HCCs. Further prospective studies with large numbers of patients are needed to fully clarify the clinical implications of tumor angiogenesis and its association with VEGFR2, PDGFR-α, and PDGFR-β.

Quantification of Microvessel Density in Hepatocellular Carcinoma with Whole-slide Digital Analysis – Its Clinical and Prognostic Significance, and Associations with PDGFR-α, PDGFR-β, and VEGFR2

By

Yuanyuan Fang

Master of Medicine, Nankai University, 2010
Bachelor of Medicine, Nankai University, 2008

Thesis Committee Chair: Roberd Bostick, MD, MPH

An abstract of
A thesis submitted to the Faculty of the
Rollins School of Public Health of Emory University
In partial fulfillment of the requirements for the degree of
Master of Public Health
In Epidemiology
2012

Table of Contents

Chapter I: Background

Hepatocellular carcinoma

Hepatocellular carcinoma (HCC) is the sixth most common cancer and third most common cause of cancer-related death (1) in the world. An estimated 748,300 new liver cancer cases and 695,900 cancer deaths occurred worldwide in 2008. Half of these cases and deaths were estimated to occur in China (1). Among primary liver cancers, HCC represents the major histological subtype, accounting for 70% to 85% of the total liver cancer burden worldwide (2). The high mortality rate is attributed primarily to the poor prognosis among patients with advanced-stage HCC. In the west and Japan, the disease is diagnosed in 30% at early stages of cases and is amenable to potentially curative treatments, such as surgical therapies (resection and liver transplantation) and locoregional procedures (radiofrequency ablation). Five-year survival rates of up to 50% can be achieved among these patients (3). However, disease that is diagnosed at an advanced stage or with progression after locoregional therapy has a dismal prognosis, due to the underlying liver disease and lack of effective treatment options.

Angiogenesis in HCC

Angiogenesis, defined as the formation of new blood vessels from existing vasculature, is a prerequisite process for tumor growth and metastasis. This process not only provides the route for nutrient supply to the tumor but also the conduit for tumor cells to be shed into the circulation. HCC is a highly angiogenic cancer. Its vasculature displays marked abnormalities (4), and is less dense than normal liver vasculature (5). HCC vessels have an abnormal blood flow and are excessively leaky. This leads to hypovascular areas and

severe hypoxia and/or necrosis. Hypoxia may promote HCC growth and progression and resistance to therapies (6). Inducing vessel normalization and alleviating hypoxia delays HCC growth (3).

Microvessel density

Tumor microvessel density (MVD), which reflects angiogenesis in tumor areas, has been found to be associated with prognosis and metastasis in many tumors, such as breast carcinoma, gastric carcinoma, colorectal carcinoma, pancreatic carcinoma, and HCC (7). However, results of studies on the prognostic value of MVD have not been homogeneous, probably because of selection bias in using different areas of tumors for study and a lack of accurate patient follow-up data in retrospective studies (8).

The normal sinusoid endothelial cell of liver is characterized by the expression of markers such as CD4, CD14 and CD32, and by the lack of expression of normal capillary endothelial markers such as CD31 and CD34. In HCC, the normal sinusoid endothelial cells lose their structural and phenotypic characteristics and adopt the structure and phenotype of normal capillary endothelial cells, which is called capillarization. This process is associated with increased expression of vascular endothelial growth factor (VEGF), basic fibroblast growth factor, and hypoxia-inducible factor 1-α, which indicates that the capillarization phenomenon is not merely a change of endothelial cell differentiation, but rather a process of tumor angiogenesis (9). CD31 and CD34 are expressed by the endothelial cells of the sinusoid-like vessels of HCC.

Most of the previous studies (10-12) use a microvessel density (MVD) assessment method first defined by Weidner (13) and then modified by Tanigawa (11). In this method, slides are first examined under 100 × magnification to identify the highest

vascular density areas within the tumor. Then five areas of highest MVD are selected under 200 × magnification (0.74 mm^2). The average counting of the five areas is recorded as the MVD level of the case. Any brown staining endothelial cell or endothelial cell cluster that is clearly separated from adjacent microvessels, tumor cells, and connective elements is considered as a single, countable microvessel regardless of whether a vessel lumen is seen. Even those distinct clusters of brown-staining endothelial cells, which might be from the same microvessel which goes in and out of the section, are considered as distinct microvessels. Also, since some of the vessels are quite large compared with the distinct clusters described above, Tanigawa modified the former method to calculate every 40 μm of the length of the large vessel as one distinct count of vessel.

Brawer et al(14) compared manual intratumor microvessel determinations with those determined by automated counting and found a very tight correlation (R^2=0.98, $p<0.001$).

CD34 is by far the preferred endothelial cell markers in many laboratories (7, 11, 12, 15, 16). The association between MVD and clinicopathological features remains controversial. Poon et al(7) found that higher MVD was associated with a low preoperative serum AFP level, tumor size ≤ 5 cm, absence of venous invasion, and absence of microsatellite lesions. El-Assal et al (17) found that higher MVD was significantly correlated with tumor capsule formation and a larger tumor size (>2 cm). Tanigawa et al(11) found that higher MVD was associated with larger tumors (>2 cm), poor differentiation (Edmondson's grade II to IV), and portal vein invasion. In contrast, Sun et al (12) and Nanashima et al(15) found that MVD was not significantly associated with any clinicopathological factors.

Also, the association between MVD and the survival outcome is not yet clear. Tanigawa et al (11) and El-Assal et al (17) found that lower MVD was associated with better disease free survival in both univariate and multivariate analyses. Conversely, Nanashima et al (15) found that lower MVD was significantly associated with lower disease-free survival but was not significantly associated with lower overall survival (the overall survival among patients with lower MVD tended to be lower).

Weidner et al (13) claimed that CD34 was a more acceptable and reproducible endothelial cell marker and indicated that CD31 cross-reacts with plasma cells and thus can obscure the microvessels in the tumors with a prominent plasma cellular inflammatory background (including HCC). However, Ding et al (18) found that both CD31 and CD34 were efficient for identifying endothelial cells. Chen et al (10) found that the median MVD count of the entire series was 34.5/field for CD31 under 200×magnification and 41.4/field for CD34. Spearman analysis in this study showed CD31 to be positively correlated with CD34 ($r=0.92$, $p<0.001$).

Vascular endothelial growth factor (VEGF), and platelet derived growth factor (PDGF)

Vascular endothelial growth factor (VEGF) and platelet derived growth factor (PDGF) are ligands that activate the receptor tyrosine kinase (RTK) pathways involved in liver oncogenic and angiogenic growth(19). Both of the ligands belong to the cystine knot-containing protein superfamily of structurally and functionally related signaling molecules.

VEGF is a critical player in HCC angiogenesis. The effects of VEGF are primarily mediated via VEGFR2 in endothelial cells.(20, 21) Tumor vessels dilate and become

leaky in response to VEGF. VEGF mediates the dissolution of the vascular basement membrane and interstitial matrix and promotes endothelial proliferation, migration and assembly into vascular networks (20). Soluble receptors for VEGF (VEGFR1 or NPR1(22)) sequester the ligands and reduce angiogenic activity. The expression of VEGF and its receptors, which include VEGFR1, VEGFR2, and VEGFR3, is elevated in HCC cell lines and tissues, as well as in the blood circulation in patients with HCC.(23, 24) The increase in VEGF expression is seen in cirrhotic and dysplastic liver tissues, suggesting a possible role for VEGF-driven angiogenesis in hepatocarcinogenesis.(17) Elevated VEGF expression is linked with high HCC tumor grade, vascular invasion, and portal vein invasion.(25-27)

It has generally been presumed that VEGF, the most extensively studied cancer therapy target among the angiogenic factors, primarily targets endothelial cells, while PDGF mainly acts on mesenchymal cells.(28) However, recent studies suggest that this distinction is not absolute and that the PDGFs can also target the former and VEGF the latter. Evidence has been found that VEGF binds to and activates PDGF receptors. There may also be additional interactions between the two signal ligands.(29, 30) Growing evidence suggests that PDGF produced by tumor epithelial cells act on endothelial cells, cancer-associated fibroblasts, pericytes and infiltrating inflammatory cells to create paracrine signaling loops that promote tumor genesis(31). Expression of PDGFR-α in liver cells is found to be high during embryonic development and then substantially declines to minimal levels in adult hepatocytes. In contrast, both HCC cell lines and resected tumors had increased expression of PDGFR-α, suggesting a role for PDGFR-α signaling in hepatocarcinogenesis.(32) Another study found that PDGFR-α expression to

have predictive value for cancer recurrence, especially in otherwise low-risk patients without pathologic microvascular invasion in their resected tumors.(33)

Sorafenib and other HCC antiangiogenic therapies

Several numbers of antiangiogenic drugs are currently being tested for the treatment of HCC. The only drug with proven survival benefit for patients diagnosed at an advanced stage or who have progressed into an advanced stage after other treatments failed is sorafenib (34, 35). Sorafenib is a multikinase inhibitor that blocks Raf signaling and VEGF, PDGF, and c-Kit. It has antiproliferative and antiangiogenic activity and delays tumor progression. In a Phase 3 trial of sorafenib in advanced HCC (SHARP study) among 602 patients, the median overall survival in the sorafenib group was 10.7 months (95% CI 9.4 -13.3) versus 7.9 months (6.8 – 9.1) in the placebo group (hazard ratio 0.69, 95% CI 0.55 -0.87; p=0.0001). Survival benefit was preceded by a delay in progression: 5.5 months for sorafenib versus 2.8 months for placebo (0.58, 0.45 – 0.74; p<0.001) (34). These findings were replicated by a randomized controlled trial in Asia (35). Safety data were reproduced in a large Phase 4 trial of sorafenib in more than 1,500 patients (21). These results have established sorafenib as the standard of care for advanced HCC.

Summary

The successfulness of Sorafenib and the recent failures or modest efficacy of other antiangiogenic agents triggered the enthusiasm for mechanistic investigations of antiangiogenetic therapies. A well-designed and standardized method is needed to evaluate the association of angiogenesis with postoperative survival, and the correlations between angiogenesis and the antiangiogenetic targets. This method could lead to a better understanding of antiangiogenic therapies based on biomarkers.

Thus, we aim to use a standardized method with whole-slide digital analysis, 1) to compare it with the traditional manually grading method, 2) to evaluate the angiogenesis measurement – two assessing methods of Microvessel density (MVD), 3) to evaluate the associations between MVD, the three Sorafenib targets (PDGFR-α, PDGFR-β, VEGFR2), and the clinicalpathologic characteristics, and 4) to evaluate the predictive values of MVD and the biomarkers.

Chapter II: Manuscript

Quantification of Microvessel Density in Hepatocellular Carcinoma with Whole-slide Digital Aanalysis – Its Clinical and Prognostic Significance, and Associations with PDGFR-α, PDGFR-β, and VEGFR2

By Yuanyuan Fang

Abstract

Aims: To investigate the following correlations/associations related to evaluations of whole-slide digital analysis of tumors in patients undergoing resections of hepatocellular carcinoma (HCC): 1) between two different methods of microvessel density (MVD) evaluation, developed by Weiss et al and Tanigawa et al, respectively; 2) between whole slide digital analysis and manual grading of expression of platelet derived growth factor receptor-α (PDGFR-α), platelet derived growth factor receptor-β (PDGFR-β), and vascular endothelial growth factor receptor 2 (VEGFR2); 3) of tumor MVD with clinicopathologic characteristics and postoperative overall survival; and 4) of PDGFR-α, PDGFR-β, and VEGFR2 expression with MVD, clinicopathologic characteristics, and postoperative overall survival.

Methods: Tumor MVD was assessed in 47 patients with resected HCC using the Aperio microvessel analysis algorithm after immunostaining for CD31. Expression of PDGFR-α, PDGFR-β, and VEGFR2 in HCCs was assessed using the Aperio positive pixel count algorithm. Patients were prospectively followed until their death.

Results: 1) We observed a good agreement between the two MVD evaluation methods (r=0.95; kappa=0.87). 2) The average intensity (the inverse of the optical density) of the

biomarker staining was most highly correlated with manual grading (r=0.69 for PDGFR-α; r=0.69 for PDGFR-β; and r=0.82 for VEGFR2). 3) Higher MVD was statistically significantly associated with a negative microscopic margin (p=0.004) and a smaller tumor size (≤5cm) (p=0.003). A higher MVD and a lower PDGFR-α expression together were the most strongly associated with a better overall survival (HR: 0.014; 95% CI: 0.001,0.23) among female patients without microvascular invasion of HCCs. 4) We found no significant associations of PDGFR-α , PDGFR-β, and VEGFR2, or MVD with the clinicopathologic characteristics.

Conclusion: There was a good agreement between the two MVD assessing methods. Higher MVD was found in small HCCs (<5cm) and HCCs with a negative microscopic margin. MVD together with PDGFR-α may be useful as a prognostic marker combination among female patients with microvascular invasion of HCCs. Further prospective studies with large numbers of patients are needed to fully clarify the clinical implications of tumor angiogenesis and its association with VEGFR2, PDGFR-α, and PDGFR-β.

Introduction

Hepatocellular carcinoma (HCC) is the sixth most common cancer and third most common cause of cancer-related death in the world (1). The high mortality rate is attributed primarily to the poor prognosis among patients with advanced-stage HCC.
In HCC, the normal sinusoid endothelial cells lose their structural and phenotypic characteristics and adopt the structure and phenotype of normal capillary endothelial cells, which is called capillarization. This process is associated with increased expression of vascular endothelial growth factor (VEGF), basic fibroblast growth factor, and hypoxia-inducible factor 1-α, which indicates that the capillarization phenomenon is not merely a

change of endothelial cell differentiation, but rather a process of tumor angiogenesis (9). Angiogenesis, defined as the formation of new blood vessels from existing vasculature, is a prerequisite process for tumor growth and metastasis. This process not only provides the route for nutrient supply to the tumor but also the conduit for tumor cells to be shed into the circulation. Tumor microvessel density (MVD), which reflects angiogenesis in tumor areas, has been found to be associated with prognosis and metastasis in many cancers, such as breast carcinoma, gastric carcinoma, colorectal carcinoma, pancreatic carcinoma, and HCC (7). However, the results of studies on the prognostic value of MVD have not been homogeneous, probably because of selection bias in using different areas of tumors for study and a lack of accurate patient follow-up data in retrospective studies (8).

Most of the previous studies (10-12) used a microvessel density(MVD) assessment method first defined by Weidner (13) and then modified by Tanigawa (11). In this method, slides are first examined under 100 × magnification to identify the highest vascular density areas within the tumor. Then five areas of highest MVD are selected under 200 × magnification (0.74 mm2). The average counting of the five areas is recorded as the MVD level of the case. Because some of the vessels are quite large, Tanigawa et al modified the method by calculating every 40 μm of a large vessel as one distinct count of vessel. As far as we know, the two methods were not compared in any study before.

The correlation between MVD and clinicopathological features remains controversial. Poon et al (7) found that higher MVD was associated with a low preoperative serum AFP level, tumor size ≤ 5 cm, absence of venous invasion, and absence of microsatellite

lesions. El-Assal et al (17) found that higher MVD was significantly associated with tumor capsule formation and a larger tumor size (>2 cm). Tanigawa et al (11) found that higher MVD was associated with larger tumors (>2 cm), poor differentiation (Edmondson's grade II to IV), and portal vein invasion. In contrast, Sun et al (12) and Nanashima et al (15) found that MVD was not significantly associated with any clinicopathological factors.

Also, the association between MVD and survival not yet clear. Tanigawa et al (11) and El-Assal et al (17) found that lower MVD was associated with better disease-free survival in both univariate and multivariate analyses. Conversely, Nanashima et al (15) found that lower MVD was significantly associated with lower disease-free survival but was not significantly associated with lower overall survival (the overall survival among patients with lower MVD tended to be lower).

Several antiangiogenic drugs are currently being tested for the treatment of HCC. The only drug with proven survival benefit for patients diagnosed at an advanced stage or who have progressed into an advanced stage after other treatments failed is sorafenib (34, 35). Sorafenib is a multikinase inhibitor that blocks Raf signaling and vascular endothelial growth factor (VEGF), platelet derived growth factor (PDGF), and c-Kit. VEGF and PDGF are ligands that activate the receptor tyrosine kinase (RTK) pathways involved in liver oncogenic and angiogenic growth (19).

VEGF mediates the dissolution of the vascular basement membrane and the interstitial matrix and promotes endothelial proliferation, migration, and assembly into vascular networks (20). Soluble receptors for VEGF (VEGFR1 or NPR1 (22)) sequester the ligands and reduce angiogenic activity. The expression of VEGF and its receptors, which

include VEGFR1, VEGFR2, and VEGFR3, is elevated in HCC cell lines and tissues, as well as in the blood circulation in patients with HCC.(23, 24) The increase in VEGF expression is seen in cirrhotic and dysplastic liver tissues, suggesting a possible role for VEGF-driven angiogenesis in hepatocarcinogenesis.(17) Elevated VEGF expression is linked with high HCC tumor grade, vascular invasion, and portal vein invasion.(25-27)

It has generally been presumed that VEGF, the most extensively studied cancer therapy target among the angiogenic factors, primarily targets endothelial cells, while PDGF mainly acts on mesenchymal cells.(28) However, recent studies suggest that this distinction is not absolute and that the PDGFs can also target the former and VEGF the latter. Evidence has been found that VEGF binds to and activates PDGF receptors. There may also be additional interactions between the two signal ligands.(29, 30) Growing evidence suggests that PDGF produced by tumor epithelial cells act on endothelial cells, cancer-associated fibroblasts, pericytes, and infiltrating inflammatory cells to create paracrine signaling loops that promote tumor genesis(31). Expression of PDGFR-α in liver cells is found to be high during embryonic development and then substantially declines to minimal levels in adult hepatocytes. In contrast, both HCC cell lines and resected tumors had increased expression of PDGFR-α, suggesting a role for PDGFR-α signaling in hepatocarcinogenesis (32). Another study found PDGFR-α expression to have predictive value for cancer recurrence, especially in otherwise low-risk patients without pathologic microvascular invasion in their resected tumors.(33)

In this study we investigated the association between tumor vascularity and the clinicopathological characteristics of 47 cases of HCC using anti-CD31 immunohistochemical staining. Cox proportional hazards model was used to clarify

whether intratumor MVD, as well as PDGFR-α, PDGFR-β, and VEGFR2 expression, were independent predictors of prognosis for patients with HCC.

Method

Data collection

Tissue samples

With the approval of the institutional review board of Emory University, we reviewed a prospectively maintained hepatobiliary surgery database at the Winship Cancer Institute at Emory University. A total of 72 patients with a diagnosis of HCC who underwent resection between August 2000 and March 2008 were selected and 52 patients were identified to have tissue available for analysis. Overall survival (OS) was ascertained by the clinical follow-up documented in each patient's record and by the Social Security Death Index. Patients who did not survive beyond 30 days after surgery (5 out of 52 patients) were not included in the study to avoid bias from perioperative morality. Thus 47 patients' tissue samples were included in this study.

Hematoxylin and eosin-stained slides were reviewed by an experienced pathologist to confirm the presence and quality of tumor and to select the appropriate tissue blocks. Sections containing both HCC and peritumoral tissues were then selected from the archived tissue.

Clinical information

Demographic data, liver function assessed by the nonadjusted model for endstage liver disease (MELD) score, date of HCC diagnosis, and types of surgery were obtained by reviewing the patients' medical charts. Important tumor factors such as tumor size,

number, presence of macro- and micro-vascular invasion, and microscopic margin were obtained from pathology reports. Patients were censored at the latest date when they were seen alive or at the date of their non-tumor-related death.

Immunohistochemistry

Immunohistochemical staining was performed on 4 μm sections obtained from formalin-fixed, paraffin-embedded tissue microarray blocks. After antigen retrieval (citrate buffer at a PH of 6.0 using an electric pressure cooker for 3 min at 12-15 pounds per square inch; at approximately 120℃), the tissue specimens were incubated with mouse monoclonal antibodies against CD31, VEGFR2 (SC-6251, Santa Cruz, CA; 1:50 dilution), PDGFR-alpha (SC-338, Santa Cruz, CA; 1:50 dilution), and PDGFR-beta (SC-339, Santa Cruz, CA; 1:50 dilution). Immunohistochemical staining was performed using Dako automated benchmark stainers (Dako Group, Carpinteria, CA). Detection was performed with labeled polymer (Dako EnVision+ dual link) for 30 min, and diaminobenzidine (DAB) was used as the chromogen. All slides were counterstained with hematoxylin.

Digital images

Each glass slide was automatically converted to the whole slide image (WSI) using the Aperio ScanScope XT (Aperio Technologies, U.S.A.). The WSIs were stored on the server of the Center for Comprehensive informatics (CCI) at Emory University. The Aperio's Image Scope software was used for remotely screening the WSIs and selecting the entire tumor area from each case excluding connective tissues and necrotic areas – by a pathologist at the workstation of the CCI. The selection of tumor areas was performed without knowledge of clinicopathologic data.

Measurements

Digital evaluation of MVD

The recorded whole slide images of each case were assessed using Aperio microvessel analysis algorithm for the average MVD, average stain intensity, average lumen area (μm^2), average vascular area (μm^2), and median vessel wall thickness (μm). MVD was defined as number of vessels per square-micron (μm). Vascular area was defined as the sum of the areas of all the endothelial cells of a vessel. Adjusted MVD as defined by Tanigawa was obtained using microvessel density × mean vessel perimeter (μm) / 40 (μm). All the variables used to evaluate MVD and the other vascular characteristics are listed in table 2-1 in the appendix.

Visual evaluation of PDGFR-α, PDGFR-β, and VEGFR2

Staining was graded according to a five-tier scale ranging from 0-4 based on the staining pattern of the majority of the stained tumor section (>50% of the tumor present on the section). Biomarker labeling was indicated by the color of the DAB. The grading standard was as follows: grade 0 - negative (no brown color), grade 1 (slight brown staining above the hematoxylin counterstain), grade 2 (medium brown staining), grade 3 (strong brown staining but less than the darkest possible brown staining observed), grade 4 (darkest possible brown staining observed). Tissues of grade 4 staining represented tumors with both high percentage and staining optical densities.

Digital evaluation of PDGFR-α, PDGFR-β, and VEGFR2

The total intensity and the number of pixels of each intensity level (strong positive, positive, weak positive, negative), and the percent of positivity were quantified using the

Aperio positive pixel count analysis algorithm. Intensity is defined as the measure of brightness of the pixel, which ranges from zero (black) to 255 (bright white). The brighter the pixel is, the larger the intensity and thus the lighter the brown stain and lower the biomarker expression. The percent of positivity was defined as the total number of positive pixels divided by total number of pixels.

Statistical analysis

Data analysis was performed using SAS 9.3. The two-side significance level was defined as $p<0.05$.

Correlation between MVD and adjusted MVD

The association between MVD and adjusted MVD was first evaluated using the Pearson correlation coefficient. Then, the samples were dichotomized by the median of MVD or adjusted MVD, and the Cohen's kappa coefficient was used to evaluate the agreement between the two variables.

Correlations between visual and digital evaluations of PDGFR-α, PDGFR-β, and VEGFR2 expression

PDGFR-α, PDGFR-β, and VEGFR2 were evaluated as continuous variables. Spearman's correlation coefficients were used to estimate the correlations between the visual evaluation and digital evaluations of PDGFR-α, PDGFR-β, and VEGFR2 expression, including percent of positivity, average intensity of strong positive pixels, average intensity of all positive pixels, and average intensity of all pixels (appendix B). The expression parameter that was mostly correlated with the visual scores was used as the

digital evaluation of PDGFR-α, PDGFR-β, and VEGFR2 expressions for subsequent analyses.

Associations between MVD and PDGFR-α, PDGFR-β, and VEGFR2, with clinicopathological characteristics

Mean MVD, adjusted MVD, PDGFR-α, PDGFR-β, and VEGFR2, according to clinicopathological characteristic categories was compared by Students' t-test. All of the continuous clinicopathological variables were dichotomized by the medians of their distributions in the study population.

Survival analysis

Patients who died within 30 days of surgery were excluded from the survival analysis. Patients who survived after 5 years were censored at the end of the fifth year. The Cox proportional hazard (PH) assumption was checked using log (-log) curves, goodness of fit tests, and extended Cox models that contained a time function of log (t). Although most log(-log) curves had certain extent of non-parallelism (Appendix D), we could not reject the proportional assumption due to the subjectivity of the method. The goodness-of-fit test is a general test to assess the fitness of the model. Thus, we relied mostly on the extended Cox models. There were only two variables with a borderline p value of 0.05 for the Wald tests of the interaction term V ×log (t): the percent of lumen area and the average intensity of PDGFR- β (Appendix B). Thus, it was decided that there was no gross violation of PH assumptions.

Univariate survival analysis was performed using the Kaplan-Meier log-rank test (for categorical variables) and with the Wald test in Cox proportional hazard models (for

continuous variables). Multivariate Cox proportional hazards models were built to identify the significant exposures, confounders, and effect modifiers (appendix B). Interaction terms were evaluated one at a time for each exposure because of the small sample size. Confounders were evaluated based on "change-in-estimate" backward elimination approach with the 10% rule (36).

Results

Correlation between MVD and adjusted MVD

MVD was strongly correlated with adjusted MVD ($r=0.95$, $p< .0001$). The inter-rater agreement of the two assessing measures was fairly high ($\kappa= 0.87$), when the subjects were dichotomized into less hypervascular and more hypervascular groups by the medians of MVD or adjusted MVD (Appendix B).

Correlations between visual and digital evaluations of PDGFR-α, PDGFR-β, and VEGFR2 expression

The average intensity of all pixels was most strongly correlated with the visual scores (PDGFR-α: $r= -0.84$, $p<0.0001$; PDGFR-β: $r= -0.65$, $p<0.0001$; VEGFR2: $r=-0.82$, $p<0.0001$) (Appendix B). Thus the average intensity of all pixels was used as digital evaluation of PDGFR-α, PDGFR-β, and VEGFR2 in the subsequent analysis.

Tumor MVD, adjusted MVD, PDGFR-α, PDGFR-β, and VEGFR2 expression according to clinicopathologic characteristics

Mean MVD and adjusted MVD values were similar according to clinicopathologic characteristics (Table 1). Mean MVD or adjusted MVD was statistically significantly greater in tumors that were smaller (≤ 5 cm) ($p=0.003$), and with a negative microscopic

margin (p=0.004). Tumor size was also statistically significantly correlated with MVD or adjusted MVD when evaluated as a continuous variable (MVD: r=-0.39, p=0.006; adjusted MVD: r=-0.40, p=0.005).

Mean MVD or adjusted MVD did not statistically significantly differ by the median vessel wall thickness dichotomized by the median. However, when the median vessel wall thickness was evaluated as a continuous variable, the Pearson's correlation coefficient for MVD was 0.31 (p=0.03), and for adjusted MVD it was 0.46 (p=0.001).

We found no statistically significant association between cirrhosis, the MELD score, microvascular invasion, VEGFR2, PDGFR-α, PDGFR-β, and MVD or adjusted MVD. We also found no statistically differences between mean VEGFR2, PDGFR-α, PDGFR-β levels according to clinicopathologic characteristics (Table 2).

Association of tumor MVD with overall postoperative survival

The 5-year overall survival rate was 8% (4/47), the 3-year overall survival rate was 21% (10/47), and the 1-year overall survival rate was 62% (29/47). A total of 27 of the 47 patients died during follow up. The average overall survival among the non-censored patients was 22.0 months (std. =21.6), and ranged from 1.5 months to 93.4 months.

The association of tumor MVD on overall postoperative survival was evaluated by comparing the overall survival between patients with low and high tumor MVD dichotomized by the median MVD value. When the entire cohort of 47 patients was analyzed, neither MVD (< 121 vs. > 121/0.74 mm2) nor adjusted MVD (<248 vs. >248/0.74 mm^2) was statistically significantly associated with overall survival (HR=0.58, Wald test p=0.17, Wilcoxon test p=.06; and HR=0.70, Wald test p=0.37,

Wilcoxon test p=.14, respectively). None of the other vascular characteristics such as the percent of lumen area, percent of vascular area, average stain intensity of CD31, and median vessel wall thickness was statistically significantly associated with the overall survival. Among the clinicopathologic factors listed in table 1, the microscopic positive margin was the only factor that was statistically significantly associated with overall survival (Wilcoxon test: p=0.001; Cox proportional hazard model: HR=5.43, p=0.004).

When tumor MVD, and all the clinicopathologic factors as listed in table 1 were entered into the Cox proportional hazars model, potential interactions between MVD and the clinicopathologic factors were evaluated one at a time. Only the interaction term of MVD ×sex was significant in the model (Wald test: p=0.02). The final model was established as log h(t)= -2.59 × MVD+ 1.69 × microscopic margin+ 0.21 ×tumor size + 0.02 ×MELD score -0.03 ×Microvascular invasion + 0.02 ×age -1.09 ×sex + 3.11 ×MVD ×sex. According to this model, 5-year risk of death after surgery among the female subjects with a higher MVD compared with lower MVD was 0.07 (95% CI: 0.01, 0.67); the corresponding risk among the male subjects was 1.68 (95% CI: 0.34, 6.34). (Figure 1)

Associations of tumor PDGFR-α, PDGFR-β and VEGFR2 expression with overall postoperative survival

The average intensity of PDGFR-α expression was found to be more strongly associated with overall survival by univariate analysis (HR=0.65, p=0.30), than were PDGFR-β (HR=0.88, p=0.75) and VEGFR2 (HR=0.99, p=0.98).

Potential interactions between these biomarkers and the clinicopathologic characteristics were evaluated one at a time in the model containing each of the biomarker as the

exposure. The only statistically significant interaction was found to be between PDGFR-α and microvascular invasion status (p=0.005). The final model was established as log h (t) = -0.15 × PDGFR-α + 1.64× microscopic margin+ 0.05 ×tumor size + 0.03 ×MELD score -0.30 ×microvascular invasion - 0.001 ×age +0.40 ×sex-13.97 × PDGFR-α×microvascular invasion. The 5-year risk of death after surgery among the positive microvascular invasion subjects with a higher PDGFR-α level compared with a lower PDGFR- α level was 5.84 (95% CI: 1.02, 33.44); the corresponding hazard ratio among the negative microvascular invasion subjects was 0.26 (95% CI: 0.07, 1.00). (Figure 2)

Neither the average intensity of VEGFR2 nor the average intensity of PDGFR-β was found to be statistically significantly associated with overall survival.

Association of tumor PDGFR-α expression combined with MVD with overall postoperative survival

When MVD, PDGFR-α, and their potential interactions with the clinicopathologic characteristics were included in the model, both of MVD and PDGFR-α and their respective interaction terms remained statistically significant. The final model was established as: log h (t) = -1.57 ×PDGFR-α -2.70 ×MVD +2.20 × microscopic margin - 1.80 ×microvascular invasion + 0.23 ×tumor size + 0.07 ×MELD score +0.02 ×age - 0.64 ×sex+3.19 ×PDGFR-α×microvascular invasion + 2.91×MVD×sex.

For the patients without vascular invasion, the 5-year risk of death after surgery among patients with a lower PDGFR-α expression was 0.21 (95% CI: 0.05, 0.89), compared with patients with a higher PDGFR-α expression; while for the patients with positive vascular invasion, the corresponding risk was 5.07 (95% CI: 0.75, 34.08). The 5-year risk ratio of death after surgery among males with higher MVD was 1.24 (95%CI: 0.34,

4.90), compared with male patients with lower MVD; while the corresponding risk ratio among female was 0.07 (95% CI: 0.01 0.63).

Discussion

In this first study using whole-slide digital analysis of the prognostic value of angiogenesis in HCC we found the following: 1) the two MVD assessment methods developed by Weidner et al and Tanigawa et al were highly correlatedand were similarly associated with overall survival among HCC patients, and the predictive value of MVD was much higher than any of the other microvascular evaluations, such as percent of lumen area, median thickness of vascular walls, percent of vascular areas, and average intesnsity of CD31 stains; 2) tumor angiogenesis as reflected by MVD was more active in HCCs ≤ 5cm and HCCs with positive microscopic margin; and 3) a higher MVD was predictive of better overall survival after resection of HCCs among females. A higher MVD and a lower PDGFR-α expression was strongly predictive among female patients without microvascular invasion of HCCs. Therefore, MVD together with PDGFR-α may be useful as a prognostic marker combination in this subset of patients.

In our study, higher MVD was significantly associated with a smaller tumor size (≤5cm) (p=0.003) and a negative microscopic margin (p=0.004). Many investigators reported that MVD was increased in larger tumors (11, 17). Only a study by Poon et al (7) reported a higher MVD in smaller HCCs (≤ 5cm) compared with larger HCCs. The authors suggested that in small HCCs, active angiogenesis in the expanding edge may be needed for a rapid phase of radial growth. Studies of tumor volume doubling time found that small HCCs have an exponential phase of rapid growth (38, 39). Another plausible explanation is that microvessel formation may diminish as the arterial vasculature

becomes better established with a progressive increase in the size of HCC (17). Also, only the study by Poon et al (7) reported a statistically significant association between a higher MVD and the absence of microsatellite tumor nodules, but it was considered that the influence of tumor size on MVD could have been confounding the influences of the other pathologic parameters on MVD, including the microscopic margin status. However, in our study, the association of MVD with margin invasion status (p=0.01) remained significant when all of the confounding variables, including tumor size, were entered into a multiple linear regression analysis, with MVD as the outcome.

In our study, higher MVD was nearly statistically significantly associated with a better prognosis in univariate survival analysis (Wilcoxon p=0.06). In the multivariable Cox proportional hazards model including MVD and the other clinicopathologic characteristics, higher MVD was also statistically significantly associated with a better prognosis in female patients. Thus, the association between a higher MVD and a better prognosis was not due to the confounding effect of negative microscopic margin status, while mean MVD was found to be greater among HCCs with negative microscopic margin status. Furthermore, this association remained significant when PDGFR-α and its interaction term (PDGFR-α × microvascular invasion) were also included in the model. This result contradicts findings in other reports (7, 11, 12, 17). Only one study investigated by Nanashima et al (15) found that a higher MVD was associated with a better prognosis. The authors explained that hypovascular HCC was difficult to detect by conventional imaging and to treat by chemoembolization or other therapy. It was found in previous studies that hypovascularity of early or sclerosing HCC did not correlate with a good response to chemoembolization, which in turn correlated with a dismal prognosis

(40, 41). However, Poon et al (7) argued that the contrast enhancement on CT scans or arteriography typically seen in large HCC reflects arterial vasculature rather than microscopic neovessels, and arterial hypervascularity was more frequent in HCCs greater than 5 cm. In our study, although a larger tumor size was strongly associated with a lower MVD, it was not statistically significantly associated with prognosis. Thus, the effect of MVD on prognosis was not confounded by tumor size, or late detections by CT scans and arteriography.

Our study differed from previous studies in four important aspects. **First**, we used whole-slide digital image analysis to minimize the interobserver variation. Digital image analysis has been applied widely in recent years because of its objectivity. Previous studies used a method defined by Weidner et.al.(8), in which the five most hyper-vascular areas under ×40 magnification are selected, then microvessel counts are performed at ×200 magnification field (0.74 mm^2). This method is limited by subjective manual selection and the small tissue area evaluated. In our study, a large peripheral tumor area with high microvascular density was selected and submitted to a network server that was able to deal with the large amount of calculations. The objectively estimated MVD based on a large tissue area could make the results more repeatable. **Second**, in this study, all of the tumor sections were tissues from peripheral areas next to tumor margins. Microvessels have been shown to be heterogeneously distributed inside the tumor (8). It has been well documented in other cancers that maximal MVD is observed near the growing edge of the tumor (8, 37). Thus, the standardized tumor sections help eliminate variations in results. **Third**, we compared the MVD estimation method defined by Weidner et.al (13), and the modified method defined by Tanigawa et al (11). The

originally defined MVD and the adjusted MVD were strongly correlated with each other (Pearson r=0.95, p<.0001). The two assessment measures have good agreement and similar predictive values for overall survival. Thus, we conclude that both of the methods provide an efficient estimate of the MVD. **Fourth**, we evaluated potential interactions of MVD with PDGFR-α, PDGFR-β, VEGFR2, and various clinicopahological characteristics. We found a higher MVD to be statistically significantly associated with better survival among females, and a lower PDGFR-α expression to be statistically significantly associated with a better overall postoperative survival among those HCCs without microvascular invasion.

Our study also had several limitations. First, although the subjects are selected from a prospectively maintained dataset, we are not aware of the sampling method. And without this information, we cannot generalize our results to the population. Second, tumor stage was not included in the survival analysis, which may be a more important predictor than merely tumor size and microvascular invasion. Third, the interaction evaluation was limited by the small sample size of the study. And the large amount of data driven analysis method may lead to statistically significant associations only by chance. Also, although tumor size has been considered in many studies as an important confounder in the association between MVD and the overall survival, it was not observed in our study. In fact, most of our sample tumors were larger than 5 cm (36/47). Thus, a larger sample size with enough samples in each stratified category is needed in future study, to evaluate the interactions between MVD, PDGFR-α, PDGFR-β, VEGFR2 and the clinicalpathologic characteristics.

In conclusion, Further prospective studies with a large number of patients are needed to fully clarify the clinical implications of tumor angiogenesis and its associations with

VEGFR2, PDGFR-α, and PDGFR-β, with a view to expand our understanding of the VEGFR2, PDGFR-α, and PDGFR-β targeted antiangiogenic drugs.

References

1. Jemal A, Bray F, Center MM, Ferlay J, Ward E, Forman D. Global cancer statistics. CA: a cancer journal for clinicians 2011;61(2):69-90.

2. Perz JF, Armstrong GL, Farrington LA, Hutin YJ, Bell BP. The contributions of hepatitis B virus and hepatitis C virus infections to cirrhosis and primary liver cancer worldwide. Journal of hepatology 2006;45(4):529-38.

3. Llovet JM, Burroughs A, Bruix J. Hepatocellular carcinoma. Lancet 2003;362(9399):1907-17.

4. Llovet JM, Real MI, Montana X, Planas R, Coll S, Aponte J, et al. Arterial embolisation or chemoembolisation versus symptomatic treatment in patients with unresectable hepatocellular carcinoma: a randomised controlled trial. Lancet 2002;359(9319):1734-9.

5. Marrero JA, El-Serag HB. Alpha-fetoprotein should be included in the hepatocellular carcinoma surveillance guidelines of the American Association for the Study of Liver Diseases. Hepatology 2011;53(3):1060-1; author reply 1061-2.

6. Villanueva A, Minguez B, Forner A, Reig M, Llovet JM. Hepatocellular carcinoma: novel molecular approaches for diagnosis, prognosis, and therapy. Annu Rev Med 2010;61:317-28.

7. Poon RT, Ng IO, Lau C, Yu WC, Yang ZF, Fan ST, et al. Tumor microvessel density as a predictor of recurrence after resection of hepatocellular carcinoma: a prospective study. J Clin Oncol 2002;20(7):1775-85.

8. Weidner N. Current pathologic methods for measuring intratumoral microvessel density within breast carcinoma and other solid tumors. Breast cancer research and treatment 1995;36(2):169-80.

9. Chebib I, Shabani-Rad MT, Chow MS, Zhang J, Gao ZH. Microvessel density and clinicopathologic characteristics in hepatocellular carcinoma with and without cirrhosis. Biomark Insights 2007;2:59-68.

10. Chen ZY, Wei W, Guo ZX, Lin JR, Shi M, Guo RP. Morphologic classification of microvessels in hepatocellular carcinoma is associated with the prognosis after resection. J Gastroenterol Hepatol 2011;26(5):866-74.

11. Tanigawa N, Lu C, Mitsui T, Miura S. Quantitation of sinusoid-like vessels in hepatocellular carcinoma: its clinical and prognostic significance. Hepatology 1997;26(5):1216-23.

12. Sun HC, Tang ZY, Li XM, Zhou YN, Sun BR, Ma ZC. Microvessel density of hepatocellular carcinoma: its relationship with prognosis. J Cancer Res Clin Oncol 1999;125(7):419-26.

13. Weidner N, Folkman J, Pozza F, Bevilacqua P, Allred EN, Moore DH, et al. Tumor angiogenesis: a new significant and independent prognostic indicator in early-stage breast carcinoma. J Natl Cancer Inst 1992;84(24):1875-87.

14. Brawer MK, Deering RE, Brown M, Preston SD, Bigler SA. Predictors of pathologic stage in prostatic carcinoma. The role of neovascularity. Cancer 1994;73(3):678-87.

15. Nanashima A, Nakayama T, Sumida Y, Abo T, Takeshita H, Shibata K, et al. Relationship between microvessel count and post-hepatectomy survival in patients with hepatocellular carcinoma. World J Gastroenterol 2008;14(31):4915-22.

16. Zhang Q, Chen X, Zhou J, Zhang L, Zhao Q, Chen G, et al. CD147, MMP-2, MMP-9 and MVD-CD34 are significant predictors of recurrence after liver transplantation in hepatocellular carcinoma patients. Cancer Biol Ther 2006;5(7):808-14.

17. El-Assal ON, Yamanoi A, Soda Y, Yamaguchi M, Igarashi M, Yamamoto A, et al. Clinical significance of microvessel density and vascular endothelial growth factor expression in

hepatocellular carcinoma and surrounding liver: possible involvement of vascular endothelial growth factor in the angiogenesis of cirrhotic liver. Hepatology 1998;27(6):1554-62.

18. Ding T, Xu J, Zhang Y, Guo RP, Wu WC, Zhang SD, et al. Endothelium-coated tumor clusters are associated with poor prognosis and micrometastasis of hepatocellular carcinoma after resection. Cancer 2011.

19. Oseini AM, Roberts LR. PDGFRalpha: a new therapeutic target in the treatment of hepatocellular carcinoma? Expert Opin Ther Targets 2009;13(4):443-54.

20. Sharma P, Saini SD, Kuhn LB, Rubenstein JH, Pardi DS, Marrero JA, et al. Knowledge of hepatocellular carcinoma screening guidelines and clinical practices among gastroenterologists. Digestive diseases and sciences 2011;56(2):569-77.

21. Lencioni R, Marrero J, Venook A, Ye SL, Kudo M. Design and rationale for the non-interventional Global Investigation of Therapeutic DEcisions in Hepatocellular Carcinoma and Of its Treatment with Sorafenib (GIDEON) study. Int J Clin Pract 2010;64(8):1034-41.

22. Gish RG, Marrero JA, Benson AB. A multidisciplinary approach to the management of hepatocellular carcinoma. Gastroenterol Hepatol (N Y) 2010;6(3 Suppl 6):1-16.

23. Poon RT, Ng IO, Lau C, Yu WC, Fan ST, Wong J. Correlation of serum basic fibroblast growth factor levels with clinicopathologic features and postoperative recurrence in hepatocellular carcinoma. American journal of surgery 2001;182(3):298-304.

24. Mas VR, Maluf DG, Archer KJ, Yanek KC, Fisher RA. Angiogenesis soluble factors as hepatocellular carcinoma noninvasive markers for monitoring hepatitis C virus cirrhotic patients awaiting liver transplantation. Transplantation 2007;84(10):1262-71.

25. Yao DF, Wu XH, Zhu Y, Shi GS, Dong ZZ, Yao DB, et al. Quantitative analysis of vascular endothelial growth factor, microvascular density and their clinicopathologic features in human

hepatocellular carcinoma. Hepatobiliary & pancreatic diseases international : HBPD INT 2005;4(2):220-6.

26. Li XM, Tang ZY, Zhou G, Lui YK, Ye SL. Significance of vascular endothelial growth factor mRNA expression in invasion and metastasis of hepatocellular carcinoma. Journal of experimental & clinical cancer research : CR 1998;17(1):13-7.

27. Zhou J, Tang ZY, Fan J, Wu ZQ, Li XM, Liu YK, et al. Expression of platelet-derived endothelial cell growth factor and vascular endothelial growth factor in hepatocellular carcinoma and portal vein tumor thrombus. Journal of cancer research and clinical oncology 2000;126(1):57-61.

28. Oseini AM, Roberts LR. PDGFRalpha: a new therapeutic target in the treatment of hepatocellular carcinoma? Expert opinion on therapeutic targets 2009;13(4):443-54.

29. Andrae J, Gallini R, Betsholtz C. Role of platelet-derived growth factors in physiology and medicine. Genes & development 2008;22(10):1276-312.

30. Ball SG, Shuttleworth CA, Kielty CM. Vascular endothelial growth factor can signal through platelet-derived growth factor receptors. The Journal of cell biology 2007;177(3):489-500.

31. Semrad TJ, Gandara DR, Lara PN, Jr. Enhancing the clinical activity of sorafenib through dose escalation: rationale and current experience. Ther Adv Med Oncol 2011;3(2):95-100.

32. Stock P, Monga D, Tan X, Micsenyi A, Loizos N, Monga SP. Platelet-derived growth factor receptor-alpha: a novel therapeutic target in human hepatocellular cancer. Molecular cancer therapeutics 2007;6(7):1932-41.

33. Zhang T, Sun HC, Xu Y, Zhang KZ, Wang L, Qin LX, et al. Overexpression of platelet-derived growth factor receptor alpha in endothelial cells of hepatocellular carcinoma associated

with high metastatic potential. Clinical cancer research : an official journal of the American Association for Cancer Research 2005;11(24 Pt 1):8557-63.

34. Llovet JM, Ricci S, Mazzaferro V, Hilgard P, Gane E, Blanc JF, et al. Sorafenib in advanced hepatocellular carcinoma. N Engl J Med 2008;359(4):378-90.

35. Cheng AL, Kang YK, Chen Z, Tsao CJ, Qin S, Kim JS, et al. Efficacy and safety of sorafenib in patients in the Asia-Pacific region with advanced hepatocellular carcinoma: a phase III randomised, double-blind, placebo-controlled trial. The lancet oncology 2009;10(1):25-34.

36. David G K. Logistic regression: a self-learning text (statistics for biology and health) 3ed ed. 2010.

37. Gasparini G, Harris AL. Clinical importance of the determination of tumor angiogenesis in breast carcinoma: much more than a new prognostic tool. Journal of clinical oncology : official journal of the American Society of Clinical Oncology 1995;13(3):765-82.

38. Okazaki N, Yoshino M, Yoshida T, Suzuki M, Moriyama N, Takayasu K, et al. Evaluation of the prognosis for small hepatocellular carcinoma based on tumor volume doubling time. A preliminary report. Cancer 1989;63(11):2207-10.

39. Ebara M, Ohto M, Shinagawa T, Sugiura N, Kimura K, Matsutani S, et al. Natural history of minute hepatocellular carcinoma smaller than three centimeters complicating cirrhosis. A study in 22 patients. Gastroenterology 1986;90(2):289-98.

40. Carr BI. Hepatic artery chemoembolization for advanced stage HCC: experience of 650 patients. Hepato-gastroenterology 2002;49(43):79-86.

41. Katyal S, Oliver JH, Peterson MS, Chang PJ, Baron RL, Carr BI. Prognostic significance of arterial phase CT for prediction of response to transcatheter arterial chemoembolization in unresectable hepatocellular carcinoma: a retrospective analysis. AJR. American journal of roentgenology 2000;175(6):1665-72.

Tables

Table 1 Mean MVD and adjusted MVD according to clinicopathologic characteristics

Variables[1]	Median (range) % (n=47)	**MVD** mean (std)	p^2	**Adjusted MVD** mean(± std)	p^2
A**ge** (years)	64 (33 - 89)				
>65	38	110 (47)	0.24	213 (85)	0.46
≤ 65	62	128 (50)		233 (92)	
Sex					
male	60	121 (50)	0.97	232 (97)	0.53
female	40	122 (47)		215 (77)	
Cirrhosis					
present	38	126 (51)	0.62	237 (97)	0.48
absent	62	119 (47)		218 (85)	
MELD score	7.5 (6.4 - 22.8)				
> 7.5	40	121 (55)	0.92	227 (98)	0.91
≤ 7.5	60	122 (45)		224 (84)	
Tumor size (cm)	7 (2 - 29)				
>5	77	110 (45)	**0.003**	205 (82)	**0.003**
≤5	23	158 (41)		291 (82)	
Microscopic margin					
present	11	64 (38)	**0.004**	119 (73)	**0.004**
absent	89	128 (45)		238 (83)	
Microvascular invasion					
present	45	110 (48)	0.14	202 (83)	0.10
absent	55	131 (47)		244 (91)	
Average intensity of VEGFR2	159 (120 - 186)				
> 159	51	114 (48)	0.26	209 (88)	0.21
≤ 159	49	130 (49)		241 (88)	
Average intensity of PDGFR- α	147 (106 - 176)				
>147	51	127 (46)	0.44	230 (80)	0.72
≤ 147	49	116 (50)		220 (99)	
Average intensity of PDGFR- β	170 (130 - 190)				
>170	49	131 (50)	0.18	210 (81)	0.23
≤ 170	51	112 (45)		241 (95)	
Median vessel wall thickness (μm)	3.14 (2.64 – 3.50)				
> 3.14	53	126 (31)	0.51	246 (62)	0.11
≤ 3.14	47	116 (63)		202 (109)	

[1] MELD score, VEGFR2, PDGFR-α, PDGFR-β and median vessel wall thickness were dichotomized by the median. [2] Students' t-test was performed to compare means. Satterthwaite p-value was used when the equality of variances are rejected; Otherwise pooled p-value was used.

Table 2 The associations between VEGFR2, PDGFR-α, PDGFR-β, and the other clinicopathological characteristics

Variables[1]	**VEGFR2**		**PDGFR-α**		**PDGFR-β**	
	mean (std)	p	mean(± std)	p	mean(± std)	p
A**ge** (years)						
>65	157 (16)	0.63	147 (18)	0.39	165 (13)	0.64
≤ 65	159 (14)		143 (17)		167 (13)	
Sex						
male	155 (16)	0.18	144 (17)	0.69	166 (13)	0.84
female	161 (14)		146 (18)		167 (13)	
Cirrhosis						
present	158 (16)	0.83	146 (17)	0.78	166 (14)	0.95
absent	157 (15)		144 (18)		166 (13)	
MELD score*						
> 7.5	155 (14)	0.25	143 (18)	0.63	166 (15)	0.77
≤ 7.5	160 (16)		146 (17)		167 (12)	
Tumor size						
>5	159 (15)	0.40	145 (16)	0.60	165 (14)	0.10
≤5	154 (16)		142 (23)		172 (8)	
Microscopic margin						
present	148 (20)	0.11	130 (18)	**0.05**	156 (20)	0.07
absent	159 (14)		146 (17)		167 (12)	
Microvascular invasion						
present	159 (15)	0.76	146 (17)	0.78	168 (12)	0.31
absent	157 (15)		144 (18)		165 (14)	
Median vessel wall thickness (μm)						
> 3.14	157 (15)	0.74	143 (17)	0.52	167 (11)	0.77
≤ 3.14	159 (16)		146 (18)		166 (15)	

Figures

Figure 1 Adjusted survival curves, stratified by MVD (dichotomized by median), among females and males.

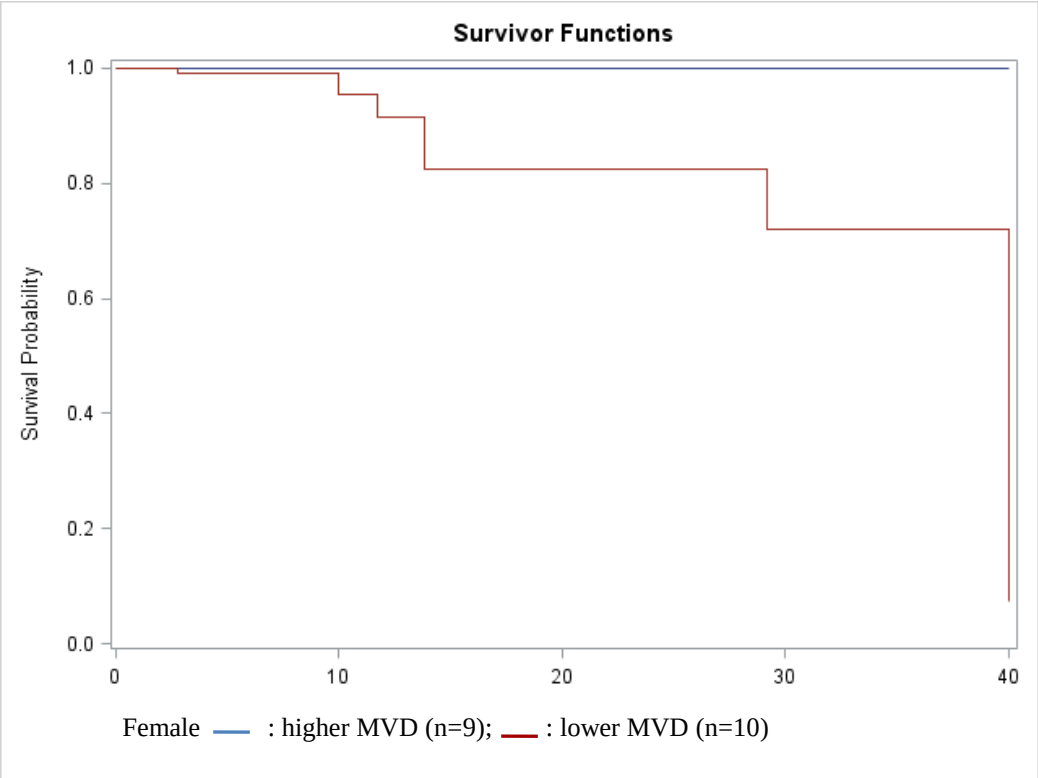

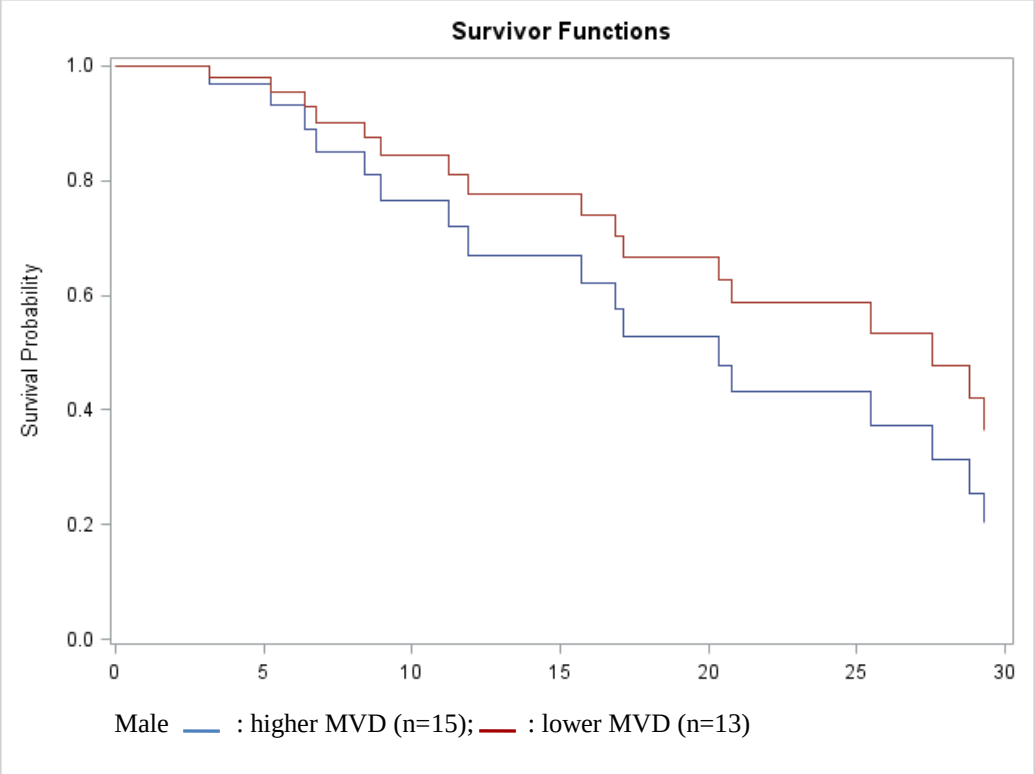

Figure 2 Adjusted survival curves, stratified by PDGFR-α expression (dichotomized by median), among patients with positive and negative microvascular invasion

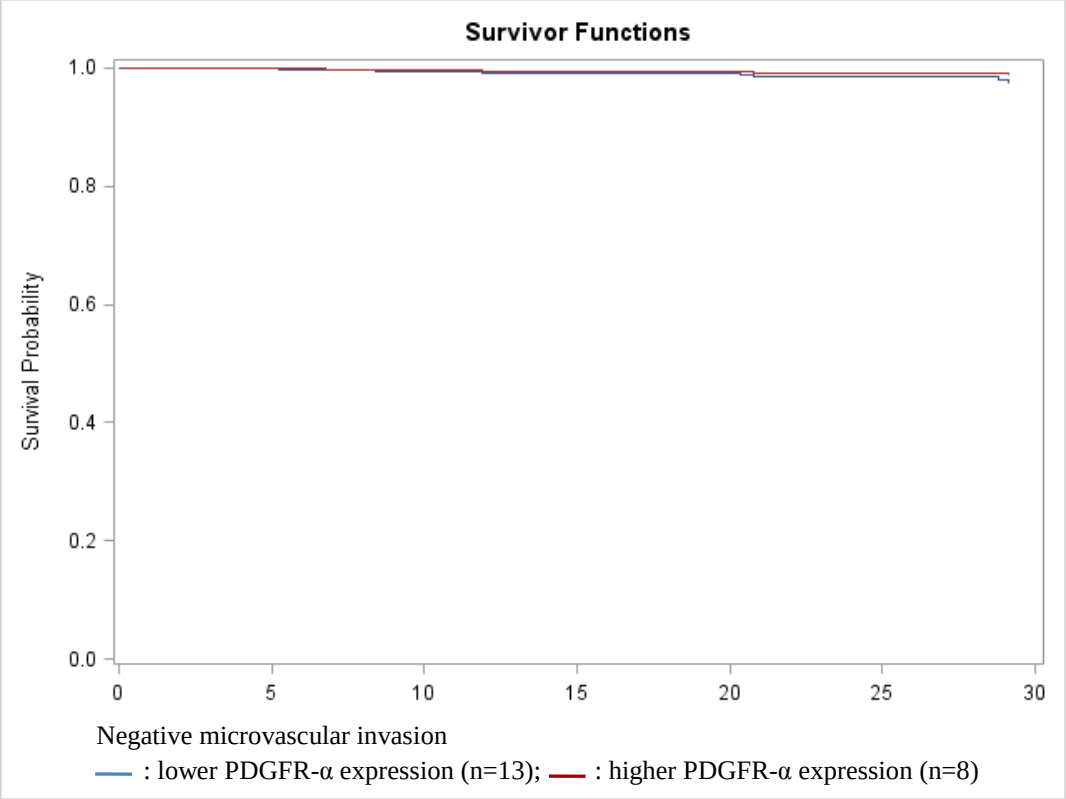

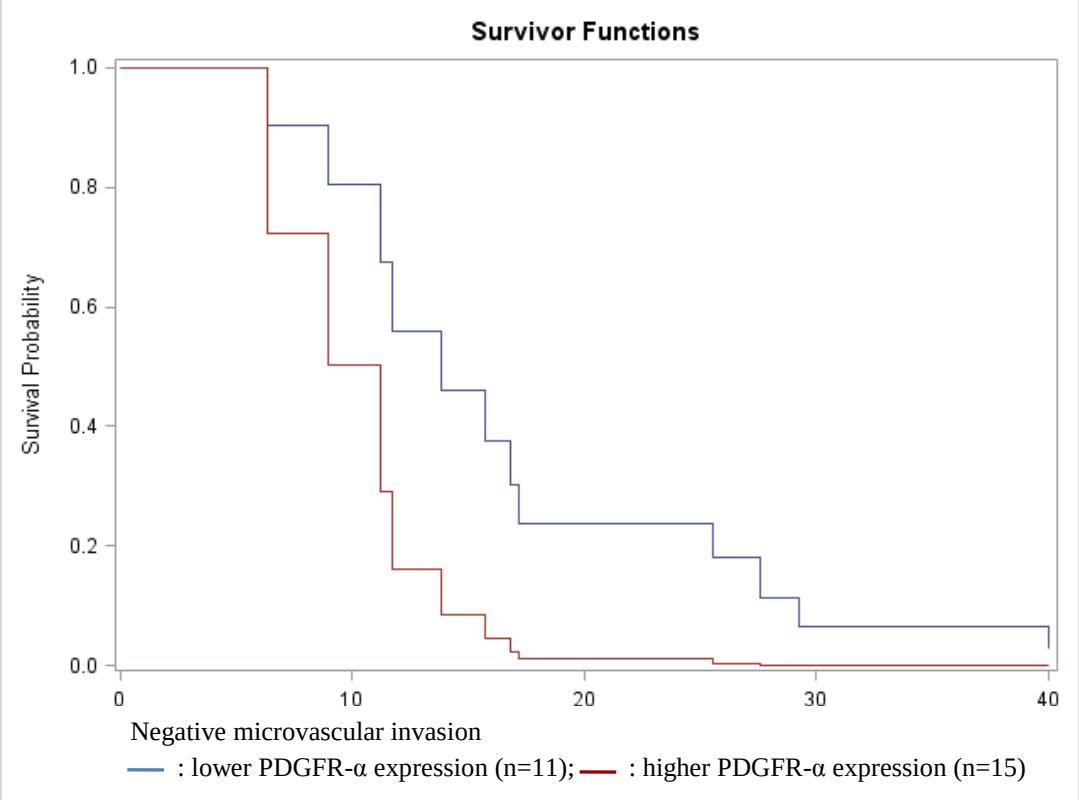

Figure 3 PDGFR-α staining of HCC, evaluated by the positive pixel count V9 algorithm (a: before analysis, at ×40 magnification; b: after analysis, at ×40 magnification)

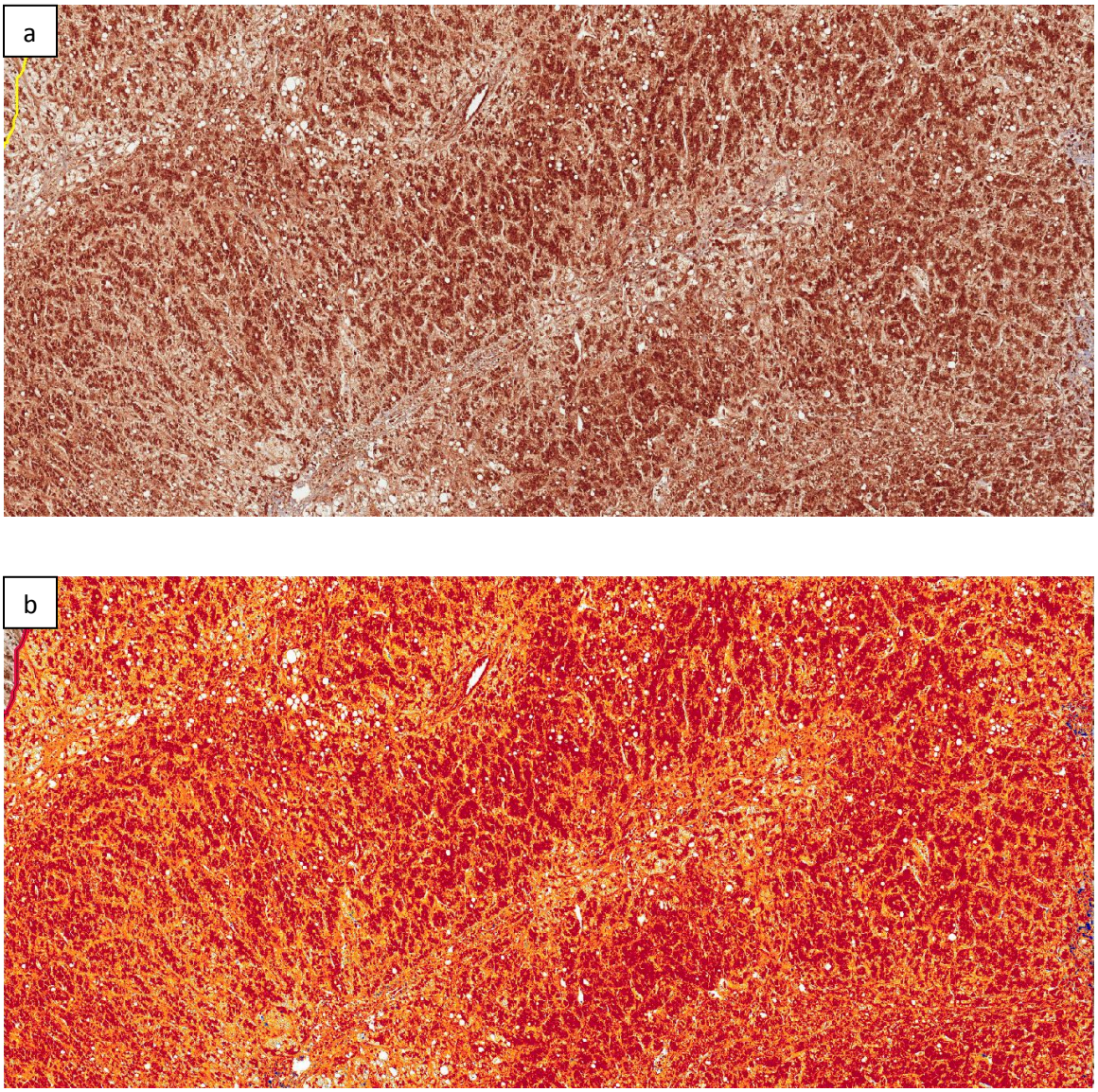

Figure 4 MVD (CD31) staining of HCC, evaluated by the microvessel analysis algorithm (a: before analysis, at ×100 magnification; b: after analysis, at ×100 magnification)

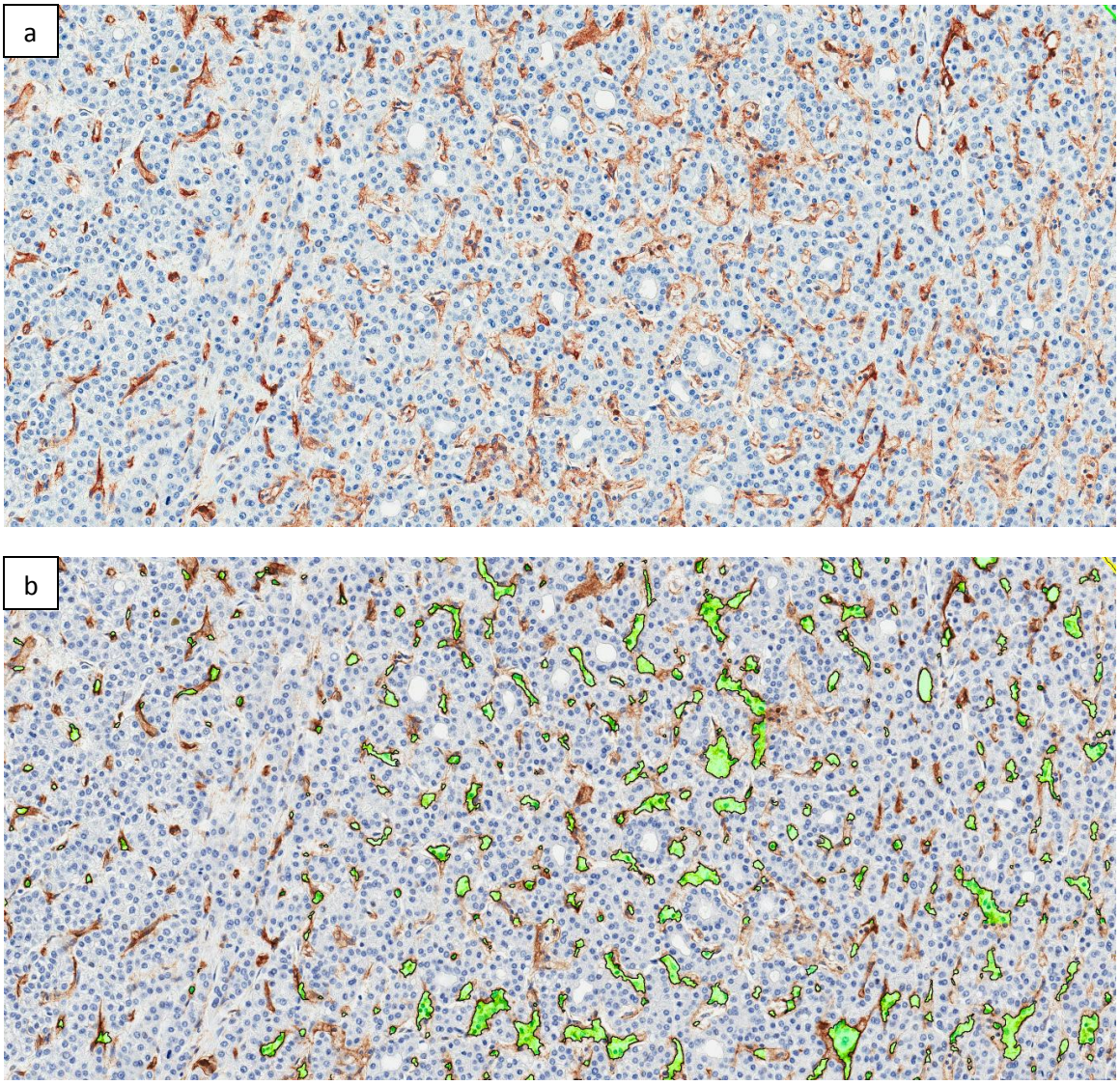

Chapter III: SUMMARY

In this study, we compared the MVD measurement method developed by Weidner et al with the modified method developed by Tanigawa et al using whole-slide digital analysis with the Aperio microvessel analysis algorithm, among a sample of 47 HCC patients. It was demonstrated that the two measurements were highly correlated with each other, and were both similarly correlated with the clinicopathologic characteristics and the postoperative overall survival among HCC patients. Also we investigated the association of the tumor expressions of the other three biomarkers: PDGFR-α, PDGFR-β, and VEGFR2, with the clinicalpathologic characteristics and the postoperative overall survival, using whole-slide digital analysis with the Aperio positive pixel count algorithm. We evaluated the potential interactions of MVD, PDGFR-α, PDGFR-β, and VEGFR2 with the cliniopathologic characteristics and found that a higher MVD was statistically significantly associated with a better overall survival among females, and a lower PDGFR-α expression (higher average intensity) was statistically significantly associated with a better overall survival among patients without microvascular invasion. These findings were limited by the small sample size of the study. And the data driven analysis method may lead us to some statistically significant associations by chance. However, we supported the association between a higher MVD and a better overall survival that has been observed only for once in a previous study, which contradicted the results of the other studies.

Although tumor size has been considered in many studies as an important confounder in the association between MVD and the overall survival, it was not observed in our study. In fact, most of our sample tumors were larger than 5 cm (36/47). Thus, a larger sample

size with enough samples in each stratified categories is needed in future study, to evaluate the interactions between MVD, PDGFR-α, PDGFR-β, VEGFR2 and the clinicalpathologic characteristics.

APPENDICES

A: MELD score

(Limquiaco, J. L., G. L. Wong, et al. (2009). "Evaluation of model for end stage liver disease (MELD)-based systems as prognostic index for hepatocellular carcinoma." J Gastroenterol Hepatol 24(1): 63-69.)

The MELD score was calculated based on the equation:

9.57 × log (creatinine mg/dL) + 3.78 × log (bilirubin mg/dL) + 11.2 × log (international normalized ratio [INR]) + 6.43

The maximal serum creatinine level considered within the MELD score equation was 4.0 mg/dL.

B: Tables

Table 2-1 The variables generated by Aperio microvessel analysis algorithm and the modified variables used for the digital evaluation of microvessel density (MVD) and other vascular characteristics.

Variables output from Aperio microvessel analysis algorithm		**Variables modified for analysis**	
Term	Definition (unit)	Term	Definition (unit)
MVD	number of vessels/μm^2	MVD	number of vessels / 0.74 mm^2
Average vessel perimeter	(μm)	Adjusted MVD	number of every 40 μm length of vessels / 0.74 mm^2
Average lumen area	(μm^2)	Directly used	
Average vascular area	average area of endothelial cells of a vessel (μm^2)	Directly used	
Average vessel wall thickness	(μm)	Directly used	

Table 2-2 The variables generated from Aperio positive pixel count analysis algorithm and the modified variables used for analysis for the digital evaluation of PDGFR-α, PDGFR-β, and VEGFR2 expression

Variables output from Aperio positive pixel count analysis algorithm		**Variables modified for analysis**	
Term	Definition	Term	Definition[1]
Percent of positivity	(%)	Directly used	
Total intensity of strong positive / positive / weak positive / negative pixels	Use default intensity cut points	Average intensity of strong positive pixels	$\frac{\text{Total intensity of sp pixels}}{\text{number of sp pixels}}$
Number of strong positive / positive / weak positive / negative pixels		Average intensity of all positive pixels	$\frac{\text{Total intensity of (sp + p + wp) pixels}}{\text{number of (sp + p + wp) pixels}}$
		Average intensity of all pixels	$\frac{\text{Total intensity of (sp + p + wp + n) pixels}}{\text{number of ((sp + p + wp + n) pixels}}$

[1]sp: strong positive, p: positive, wp: weak positive, n: negative

Table 2-3 Variables used for multivariable survival analysis

Variable categories	**Variables**
Exposures	Microvessel density PDGFR-α - average intensity of all pixels PDGFR-β - average intensity of all pixels VEGFR2 - average intensity of all pixels
Outcome measurement	Overall survival
Relevant prognostic factors	Tumor size, resection margin, microvascular invasion, MELD score, age, sex

Table 3-1 The agreement between MVD and adjusted MVD

MVD (n, %)	Adjusted MVD (n, %)		Kappa
	Less hypervascular	More hypervascular	
Less hypervascular	22 (96%)	1 (4%)	0.87 (SE: 0.14)
More hypervascular	2 (4%)	22 (96%)	

Table 3-2 Correlations between visual scoring and whole-slide digital evaluations

Pearson correlation coefficient (p-value)		Digital evaluation			
		Percent of all positive pixels	Average intensity of strong positive pixels[1]	Average intensity of all positive pixels	Average intensity of all pixels
Visual evaluation	PDGFR- α	0.57 (<0.0001)	-0.55 (<0.0001)	-0.70 (<0.0001)	**-0.69 (<0.0001)**
	PDGFR-β	0.52 (0.0004)	-0.09 (0.54)	-0.63 (<0.0001)	**-0.65 (<0.0001)**
	VEGFR2	0.76 (<0.0001)	-0.65 (<0.0001)	-0.80 (<0.0001)	**-0.82 (<0.0001)**

[1]the default value in the algorithm was used to define strong positive pixels.

Table 3-3 Correlations (Pearson) between MVD / adjusted MVD and continuous clinicopathologic variables and biomarkers

Variables	MVD		Adjusted MVD	
	r	p	r	p
Age	-0.06	0.68	-0.02	0.91
MELD score	-0.004	0.98	0.05	0.75
Tumor size	-0.39	**0.006**	-0.40	**0.005**
Average intensity of VEGFR2	-0.17	0.25	-0.16	0.27
Average intensity of PDGFR-α	0.11	0.45	0.03	0.85
Average intensity of PDGFR-β	0.12	0.43	0.13	0.39
Median vessel wall thickness	0.31	**0.03**	0.46	**0.001**

Table 3-4 Univariate analysis and Cox proportional hazards diagnostics

Variables	Univariate analysis		Proportional hazard assumption diagnostics		
	Wilcoxon test[1]	Cox proportional hazard model[2]	Log-log curves[3]	Goodness of fit test	Extended cox model (V, V × log(t))
	p-value	p-value		p-value	p-value
MVD	**0.06**	**0.14**	V	0.30	0.08
Adjusted MVD	0.14	0.37	V	0.17	0.07
Percent of lumen area	0.53	0.95	V	0.32	0.15
Percent of vascular area	0.45	0.67	V	0.14	**0.05**
Average stain intensity of CD31	0.19	0.50	V	0.87	0.71
Median vessel wall thickness	0.78	0.53	V	0.64	0.52
Average intensity of PDGFR-α	0.58	**0.07**	V	0.41	0.28
Average intensity of PDGFR-β	0.36	0.31	V	**0.01**	**0.05**
Average intensity of FLK	0.71	0.97	V	0.98	0.88
Sex	0.32	0.22	V	0.57	0.32
Age	0.26	0.27	NV	0.34	0.20
MELD score	0.59	**0.13**	V	0.51	0.73
Tumor size	0.63	0.81	V	0.70	0.48
Margin	**0.001**	**0.004**	NV	0.84	0.75
Micro-vessel	0.99	0.95	V	0.93	0.82

[1] All of the continuous variables were dichotomized by median except for tumor size (≥5 cm, < 5 cm); [2] Use continuous variables; [3] V means gross violation of parallelism, NV means no gross violation of parallelism

Table 3-5. Evaluations of potential interactions involving MVD

Variables	Interaction term	Wald test p-value
MVD (exposure)		
Microscopic margin	MVD ×microscopic margin	----[1]
Tumor size	MVD ×tumor size	0.99
MELD score	MVD ×MELD score	0.29
Microvascular invasion	MVD ×Microvascular invasion	1.00
Age	MVD ×age	0.30
Sex	MVD ×sex	0.02

[1]One of the strata had a group number of 0 and thus could not be tested.

Table 3-6. Confounding evaluation of the multivariable model contains the exposure of MVD

Wald test p-value	Golden model	Drop Microvascular invasion	Drop MELD score	Drop Tumor size	Drop age
Sex=female (n=19)	HR: 0.075 (0.008, 0.675)	HR: 0.074 (0.008, 0.667)	HR: 0.075 (0.008, 0.672)	HR: 0.080 (0.009, 0.697)	HR: 0.103 (0.012, 0.860)
Sex=male (n=28)	HR: 1.68 (0.44, 6.34)	HR: 1.70 (0.48, 5.99)	HR: 1.82 (0.56, 5.83)	HR: 1.92 (0.60, 6.15)	HR: 1.97 (0.62, 6.25)
MVD	0.02	0.02	0.02	0.02	0.04
Sex	0.13	0.1	0.09	0.10	0.18
MVD ×sex	0.02	0.01	0.01	0.01	0.006
Microscopic margin	0.05	0.05	0.02	0.02	0.02
Age	0.32	0.31	0.29	0.29	
Tumor size	0.75	0.75	0.68		
MELD score	0.79	0.78			
Microvascular invasion	0.95				

Table 3-7. Evaluations of potential interactions involving VEGFR2

Variables	Interaction term	Wald test p-value
VEGFR2 (exposure)		
Microscopic margin	VEGFR2 ×microscopic margin	0.37
Tumor size	VEGFR2 ×tumor size	0.31
MELD score	VEGFR2 ×MELD score	0.98
Microvascular invasion	VEGFR2 ×Microvascular invasion	0.10
Age	VEGFR2 ×age	0.62
Sex	VEGFR2 ×sex	0.92

Table 3-8. Evaluations of potential interactions involving PDGFR-α

Variables	Interaction term	Wald test p-value
PDGFR-α (exposure)		
Microscopic margin	PDGFR-α×microscopic margin	0.99
Tumor size	PDGFR-α×tumor size	0.65
MELD score	PDGFR- α×MELD score	0.45
Microvascular invasion	PDGFR- α×Microvascular invasion	0.005
Age	PDGFR- α×age	0.16
Sex	PDGFR- α×sex	0.38

Table 3-9 Confounding evaluation of the multivariable model contains the exposure of PDGFR-α

Wald test p-value	Golden model	Drop age	Drop Tumor size	Drop MELD score	Drop sex
(Microvascular invasion=positive)	HR: 5.84 (1.02, 33.44)	HR: 5.70 (1.03, 31.51)	HR: 5.54 (1.00, 30.81)	HR: 5.44 (1.01, 29.46)	HR: 4.85 (0.89, 26.45)
(Microvascular invasion=negative)	HR: 0.26 (0.07, 1.00)	HR: 0.26 (0.07, 0.98)	HR: 0.25 (0.07, 0.97)	HR: 0.27 (0.07, 1.01)	HR: 0.30 (0.08, 1.09)
PDGFR-α	0.05	0.05	0.04	0.05	0.04
Microvascular invasion	0.02	0.02	0.02	0.02	0.18
PDGFR-α × Microvascular invasion	0.005	0.005	0.005	0.006	0.006
Microscopic margin	0.009	0.008	0.008	0.002	0.02
Sex	0.23	0.20	0.18	0.18	
MELD score	0.56	0.53	0.44		
Tumor size	0.72	0.72			
Age	0.87				

Table 3-10. Evaluations of potential interactions involving PDGFR-β

Variables	Interaction term	Wald test p-value
PDGFR-β (exposure)		
Microscopic margin	PDGFR-β×microscopic margin	0.39
Tumor size	PDGFR-β×tumor size	0.65
MELD score	PDGFR-β×MELD score	0.19
Microvascular invasion	PDGFR-β×Microvascular invasion	0.15
Age	PDGFR-β×age	0.29
Sex	PDGFR-β×sex	0.25

Table 3-11 Evaluation of potential interactions involving MVD with PDGFR-β and VEGFR2

Interaction between MVD and PDGFR-β			**Interaction between MVD and VEGFR2**		
Variables	β	p-value	Variables	β	p-value
MVD	-2.36	0.04	MVD	-1.85	0.18
PDGFR- β	0.25	0.75	VEGFR2	0.97	0.22
Sex	-0.94	0.26	Sex	-0.84	0.19
PDGFR-β ×MVD	-0.20	0.84	VEGFR2 ×MVD	-0.61	0.60
MVD ×sex	3.00	0.03	MVD ×sex	3.06	0.02
Margin	1.81	0.04	Margin	2.59	0.02
MELD	0.03	0.68	MELD	0.02	0.75
Tumor size	0.15	0.82	Tumor size	0.28	0.69
Microvascular invasion	-0.12	0.82	Microvascular invasion	-0.08	0.88

Table 3-12 Confounding evaluation of the multivariable model contains the exposure of PDGFR-α and MVD

Wald test p-value		**Golden model**	**Drop tumor size**	**Drop Tumor age**
Higher MVD & Higher PDGFR-α **VS** Lower MVD & Lower PDGFR-α	Male Positive microvascular invasion (4 vs 10)	HR: 6.26 (0.94, 53.10)	HR: 6.25 (0.92, 53.96)	**HR: 5.23** (0.69, 39.69)
	Female Positive microvascular invasion (2 vs 5)	HR: 0.34 (0.02, 6.80)	HR: 0.33 (0.02, 6.55)	HR: 0.35 (0.02, 6.51)
	Male Negative microvascular invasion (5 vs 9)	HR: 0.26 (0.03, 1.87)	HR: 0.26 (0.04, 1.88)	HR: 0.22 (0.03, 1.61)
	Female Negative microvascular invasion (2 vs 12)	**HR: 0.014 (0.001, 0.23)**	HR: 0.014 (0.001, 0.23)	HR: 0.015 (0.02, 0.85)
Higher MVD VS Lower MVD	Male (14 vs 14)	HR: 1.24 (0.31, 4.90)	**HR: 1.29** (0.34, 4.96)	
	Female (7 vs 12)	**HR: 0.07 (0.01, 0.63)**	HR: 0.07 (0.01, 0.64)	
Higher PDGFR-α VS Lower PDGFR-α	Positive microvascular invasion (13 vs 8)	HR: 5.07 (0.75, 34.08)	HR: 4.82 (0.72, 32.24)	
	Negative microvascular invasion (11 vs 15)	**HR: 0.21 (0.05, 0.89)**	HR: 0.20 (0.05, 0.85)	
	PDGFR-α	**0.03**	0.03	0.02
	MVD	**0.02**	0.02	0.02
	Microvascular invasion	0.06	0.07	0.06
	Sex	0.36	0.37	0.56
	PDGFR-α×Microvascular invasion	**0.006**	0.01	0.01
	MVD×Sex	**0.03**	0.02	0.03
	Microscopic margin	0.04	0.04	0.03
	MELD score	0.40	0.33	0.24
	Age	0.41	0.41	
	Tumor size	0.74		

[1]The hazard ratio of a group with both higher PDGFR-α and lower MVD, compared with others

C: Figures

Figure 1 Adjusted survival curves stratified by dichotomized PDGFR-β

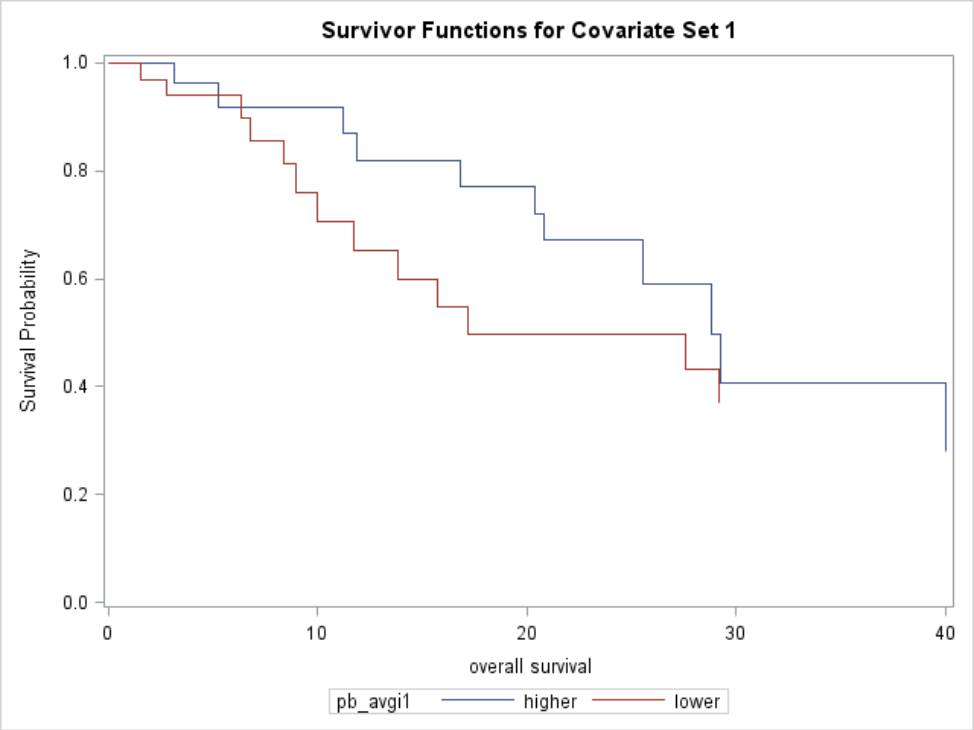

Figure 2 Adjusted survival curves stratified by dichotomized VEGFR2

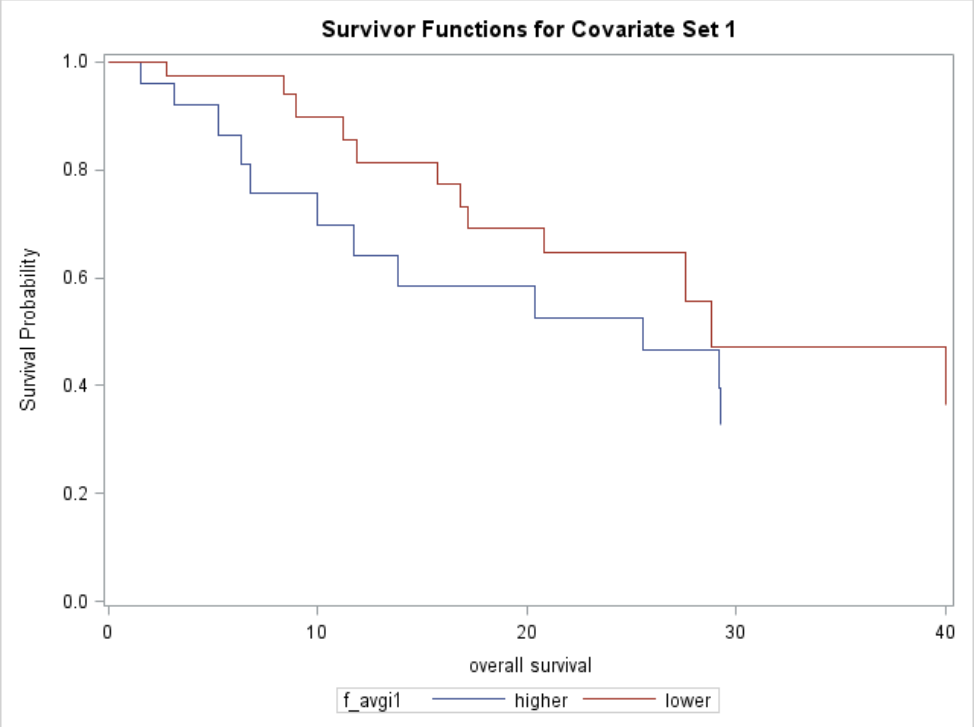

Figure 3 PDGFR-β staining of HCC, evaluated by the positive pixel count V9 algorithm (a: before analysis, at ×40 magnification; b: after analysis, at ×40 magnification)

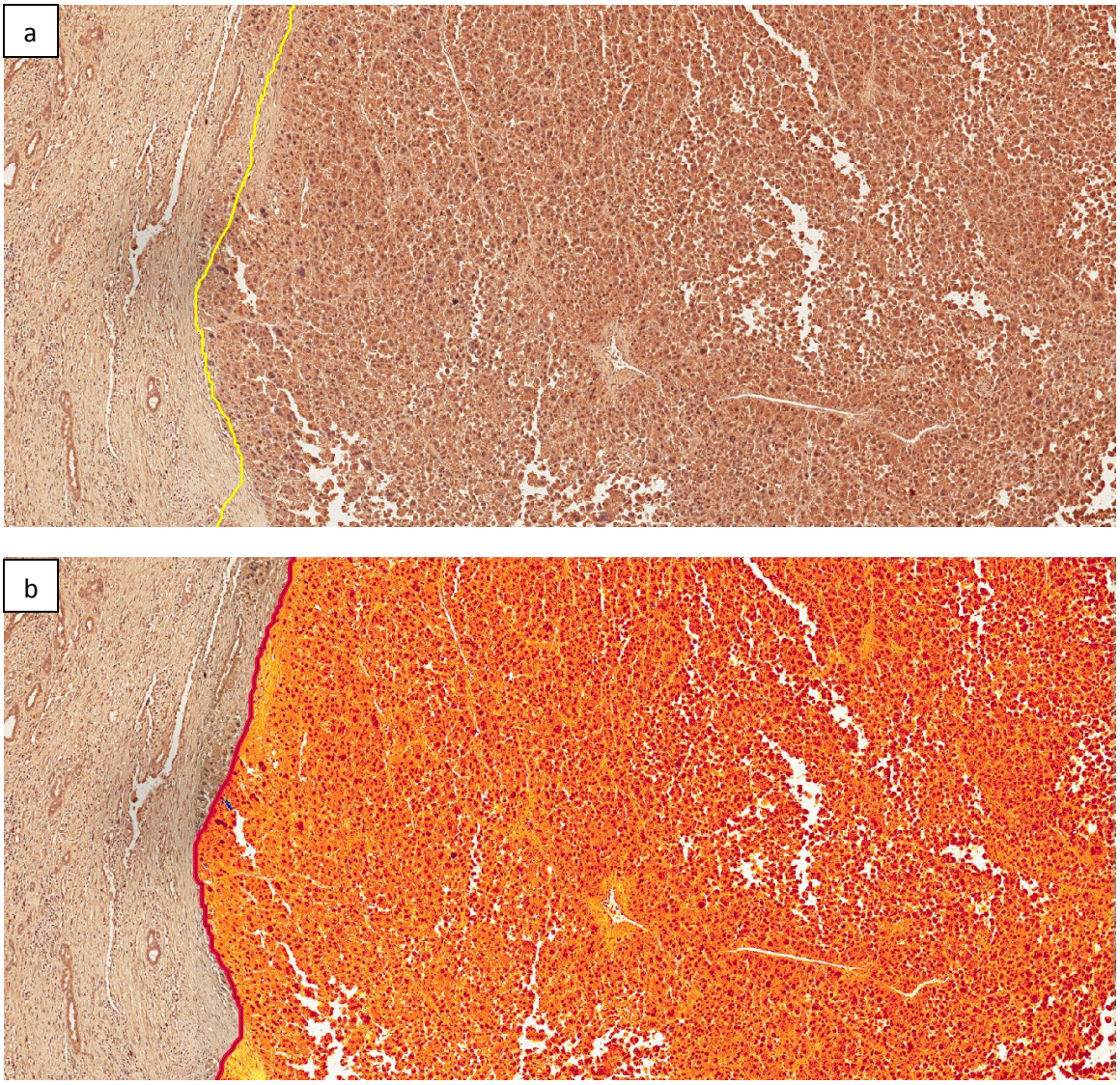

Figure 4 VEGFR2 staining of HCC, evaluated by the positive pixel count V9 algorithm (a: before analysis, at ×40 magnification; b: after analysis, at ×40 magnification)

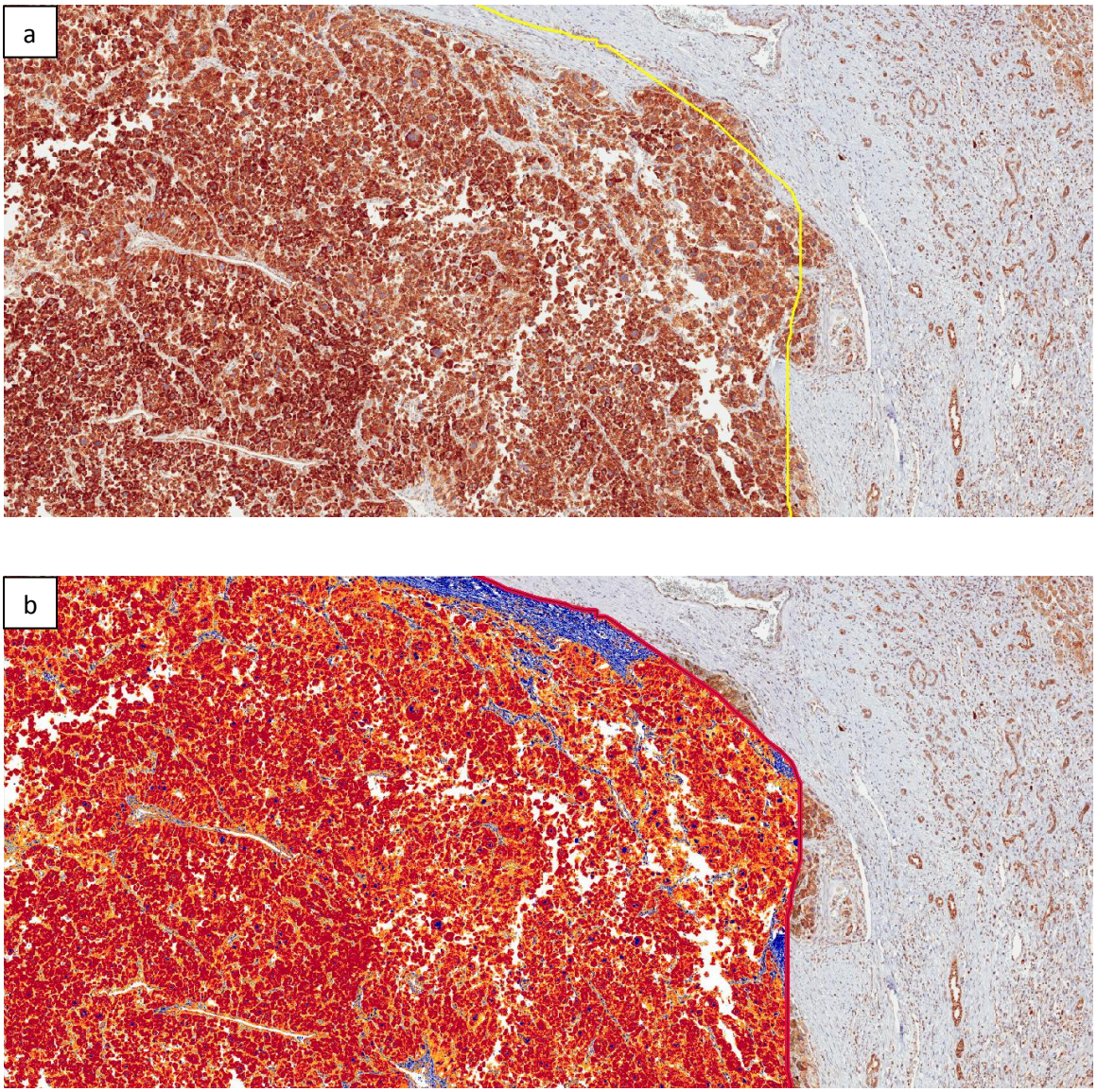

D: Proportional hazards regression diagnostics (univariate survival curves and log-log curves)

1. MVD

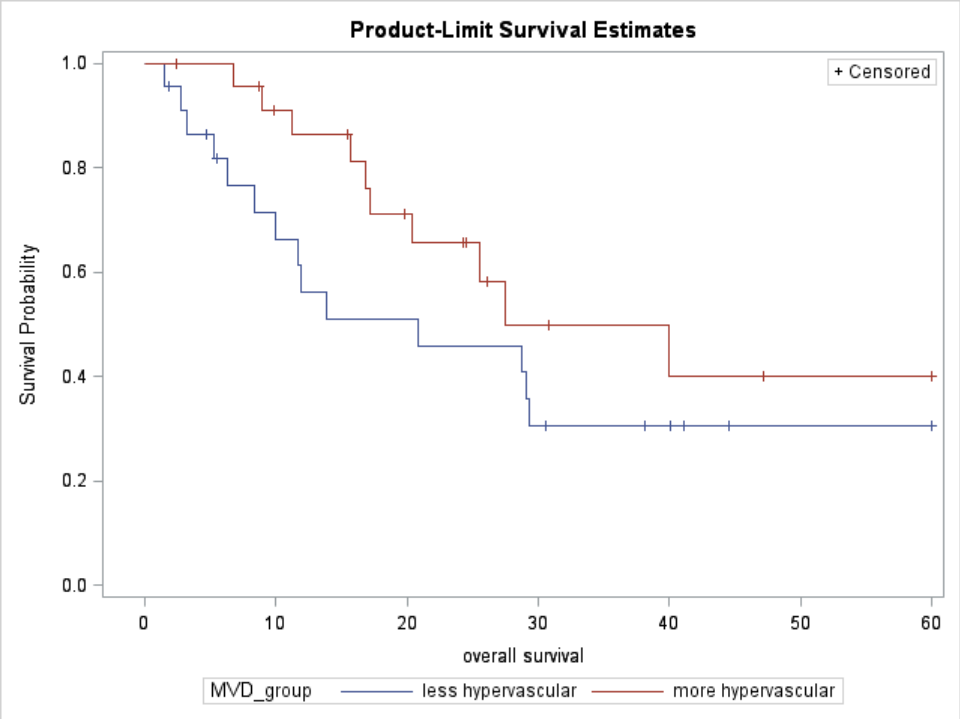

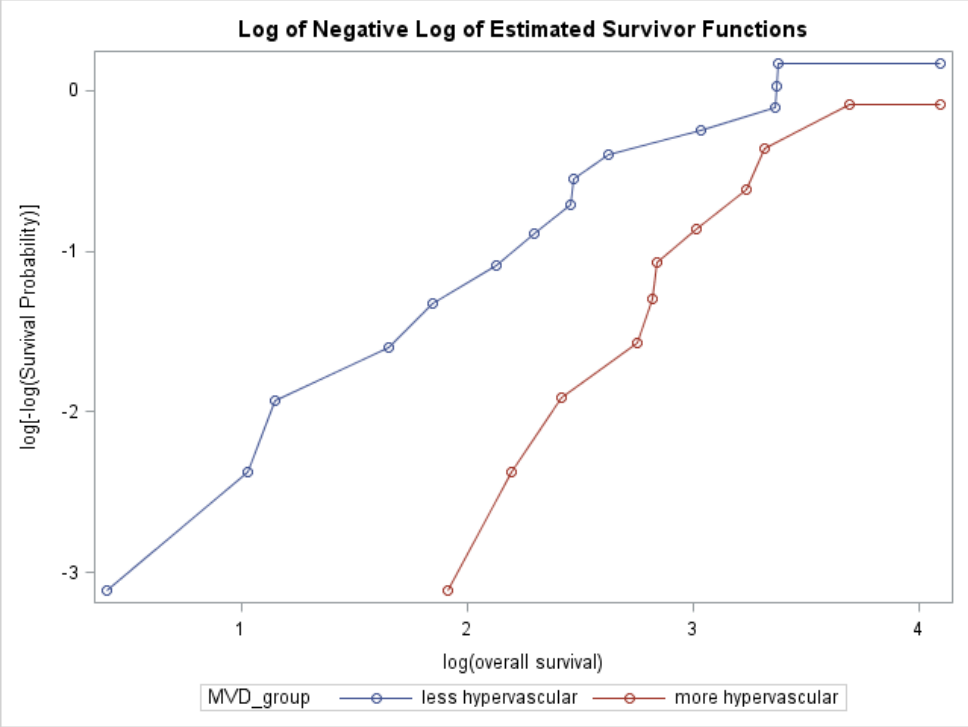

2. Adjusted MVD

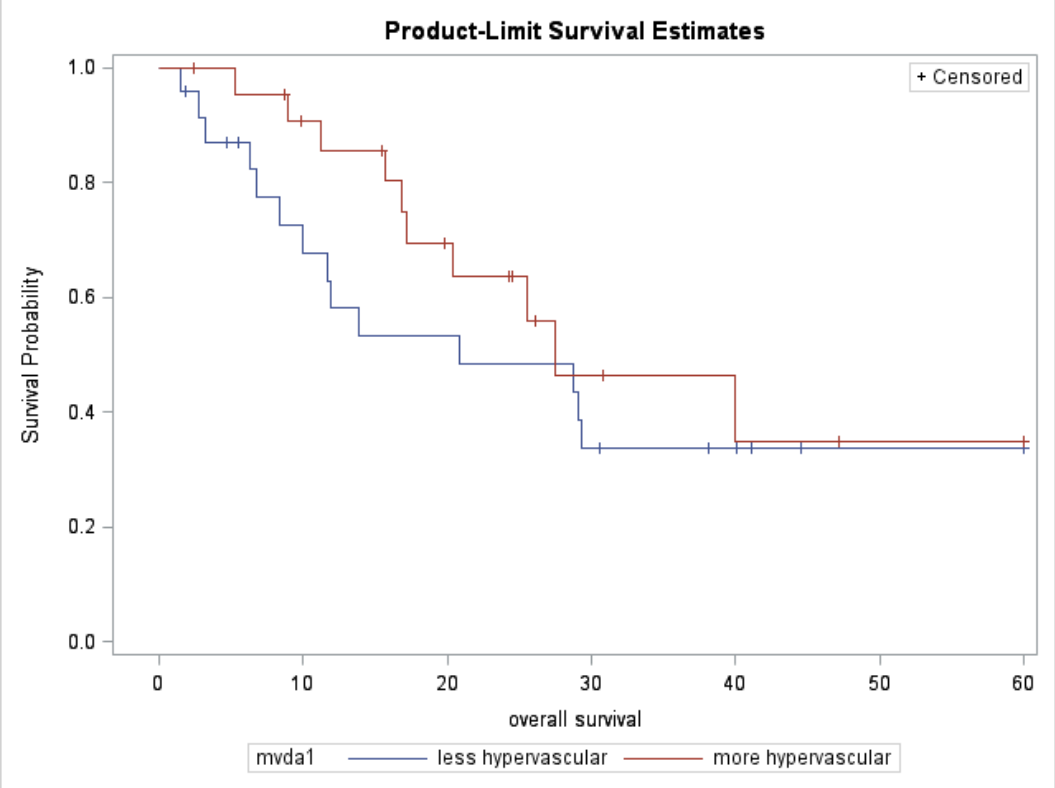

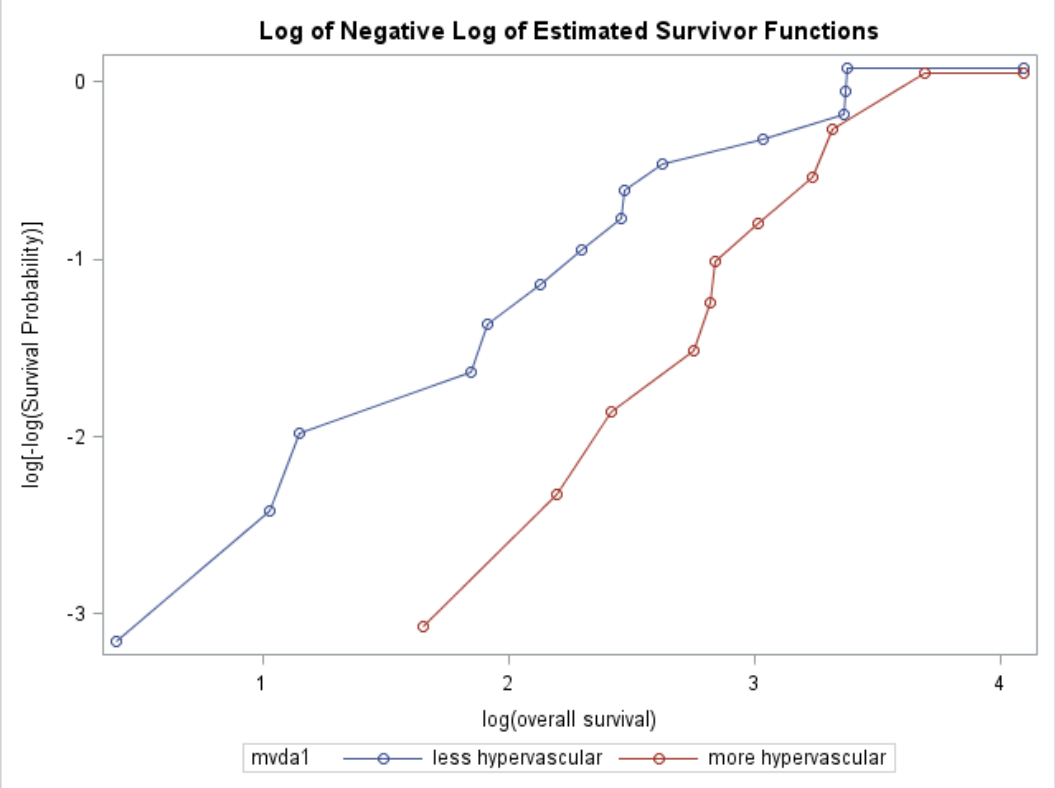

3. Average lumen percentage

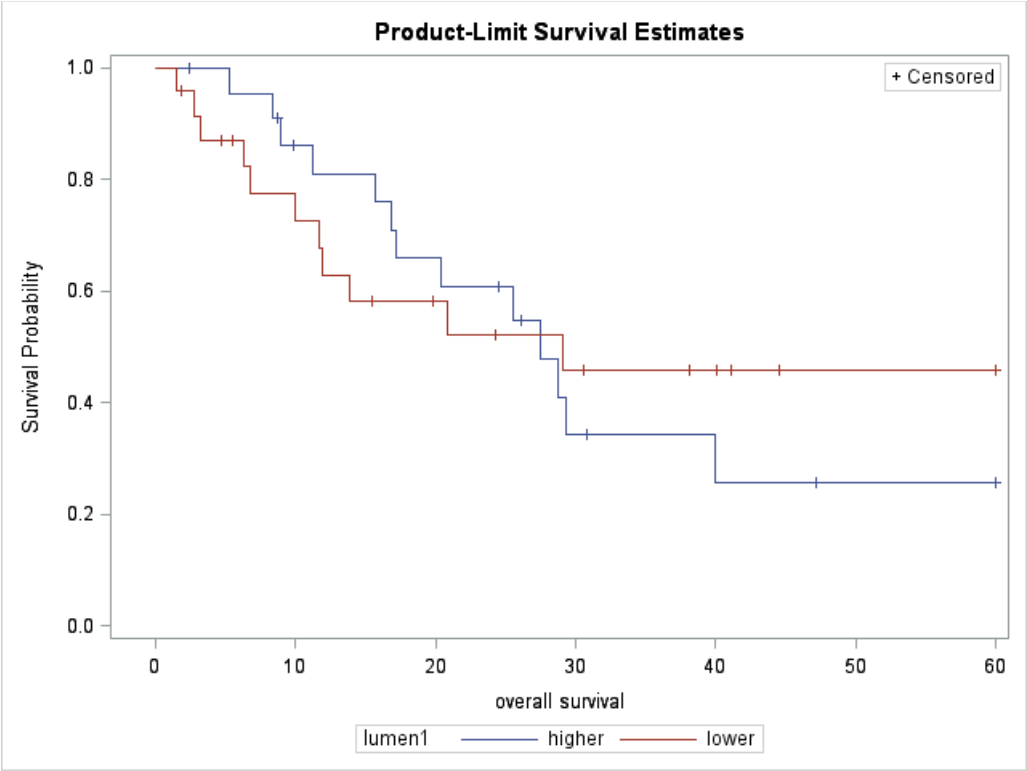

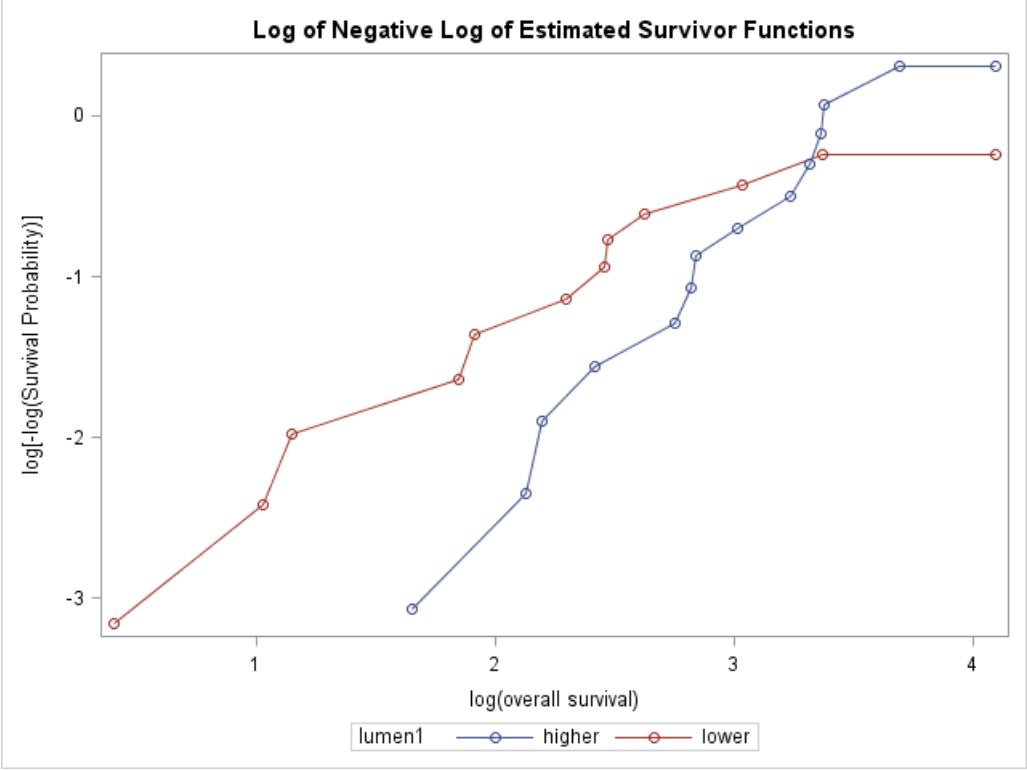

4. Vascular area percentage

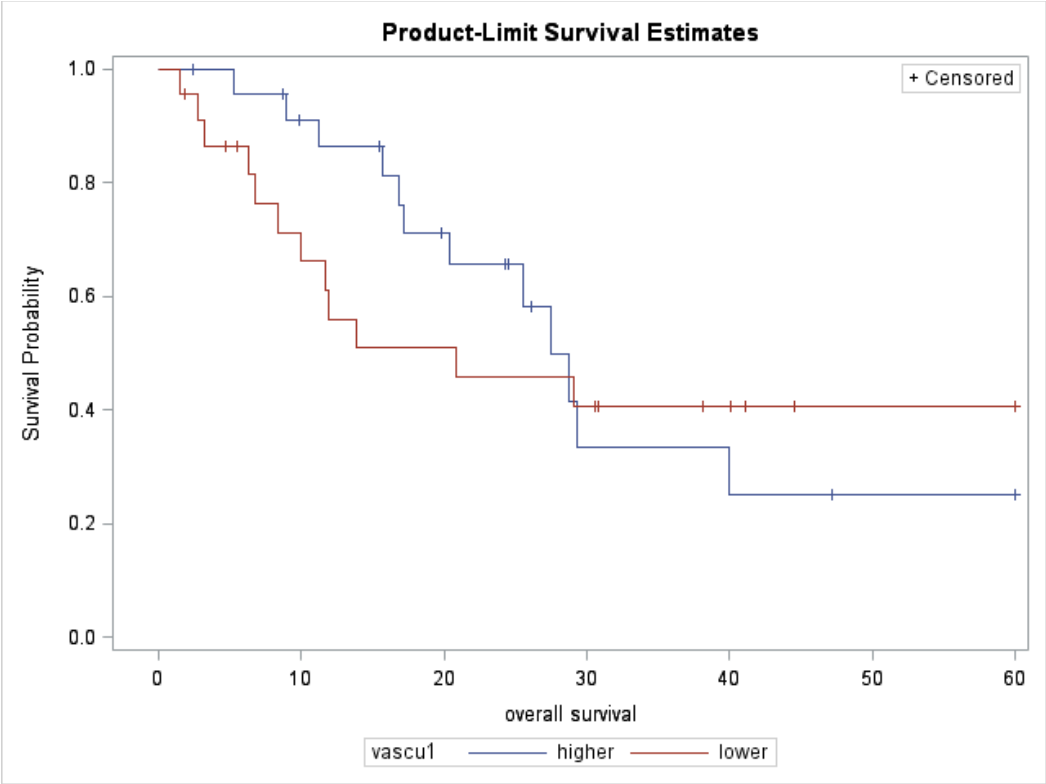

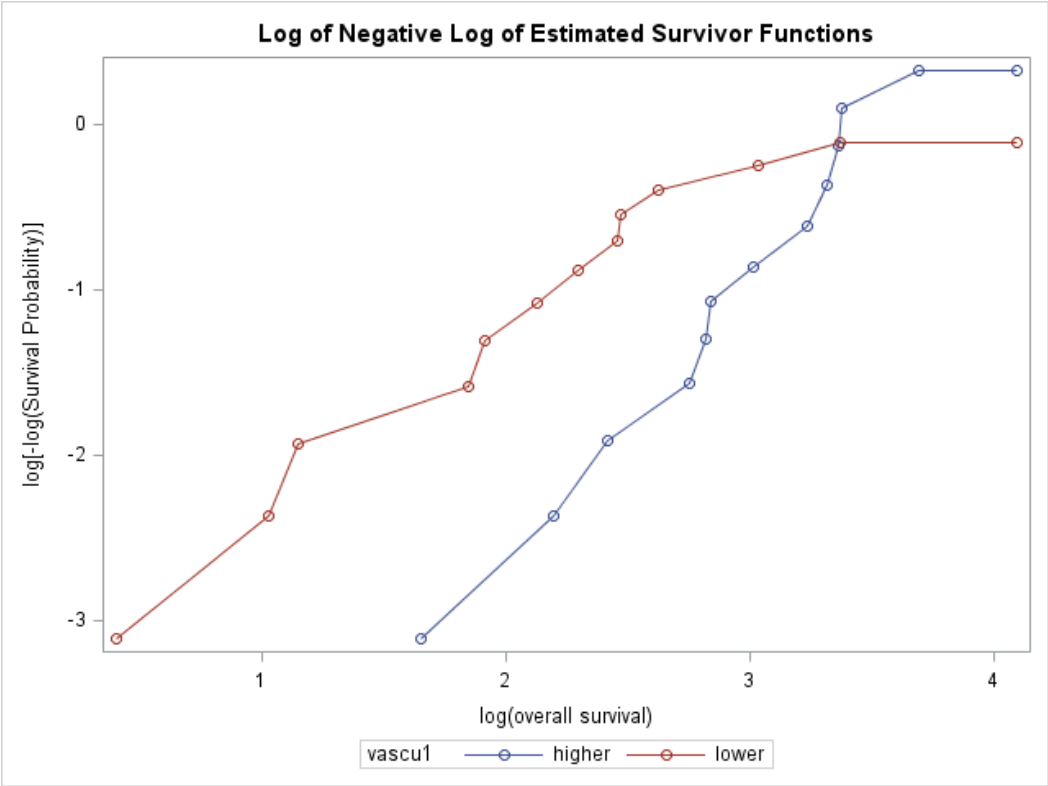

5. Average intensity of CD31

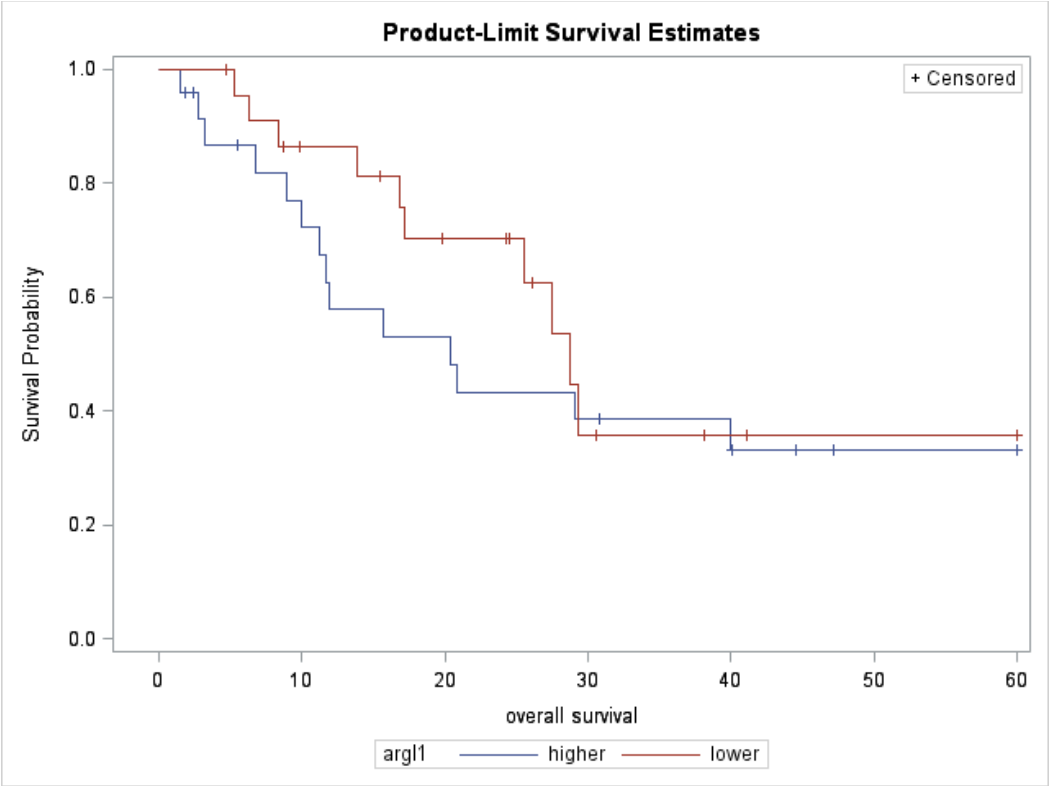

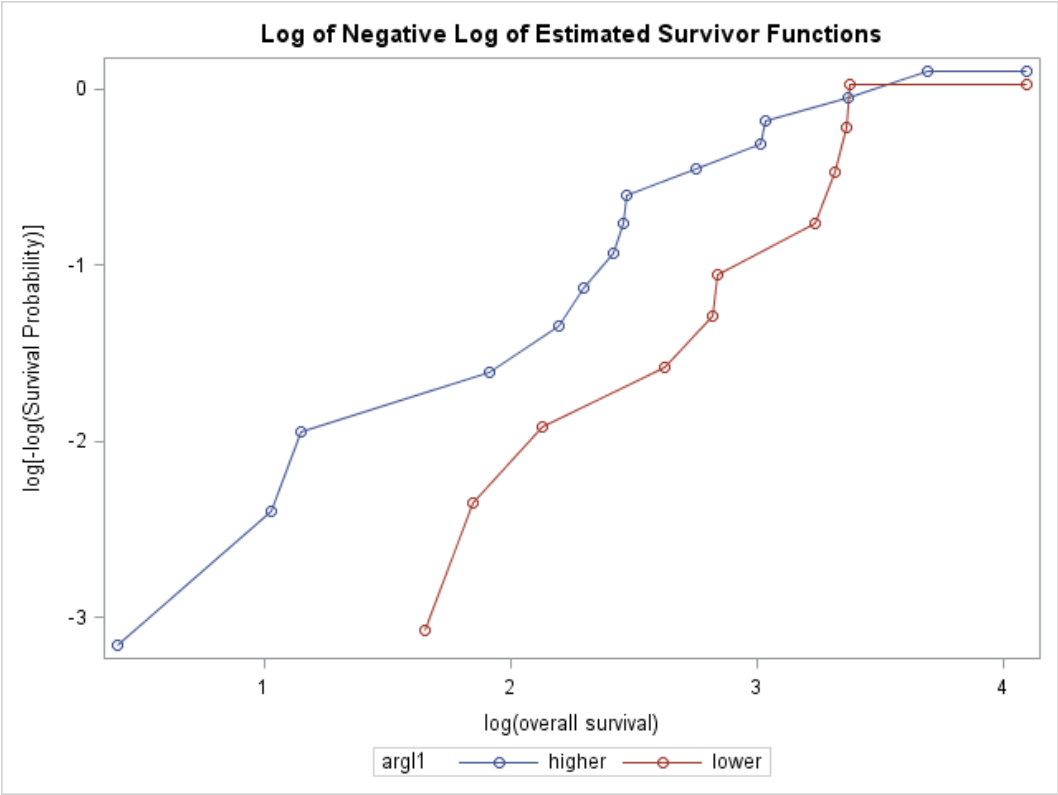

6. Median wall thickness

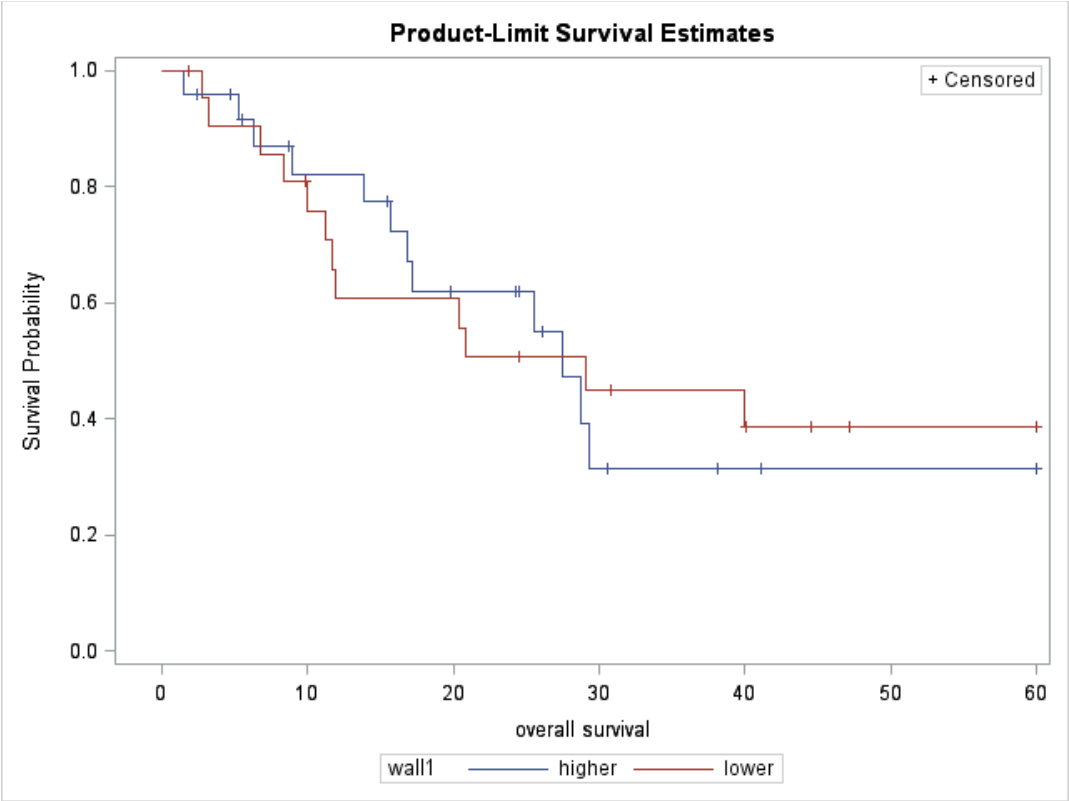

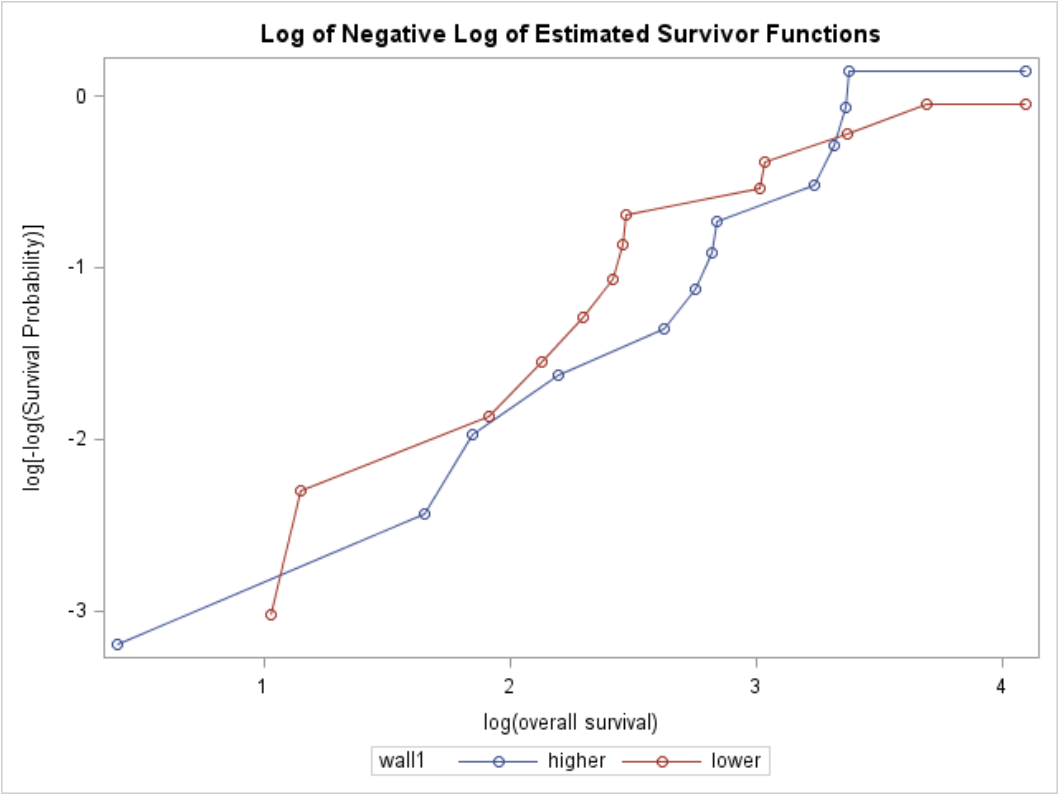

7. Age

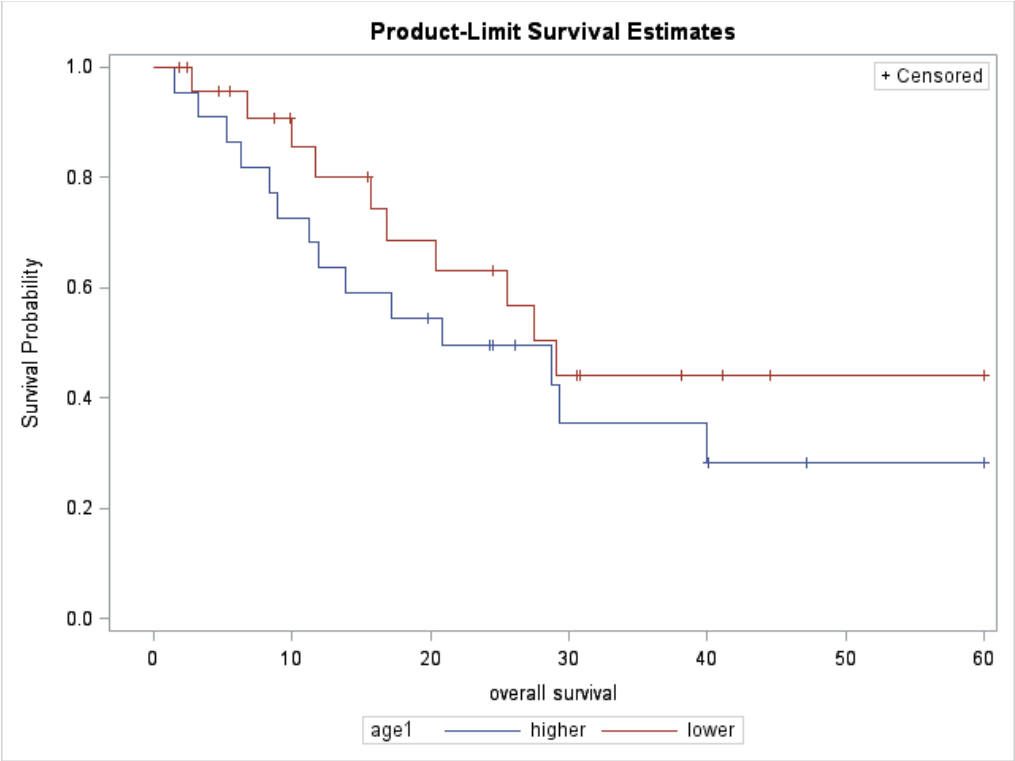
Product-Limit Survival Estimates
+ Censored
Survival Probability
1.0
0.8
0.6
0.4
0.2
0.0
0
10
20
30
40
50
60
overall survival
age1
higher
lower

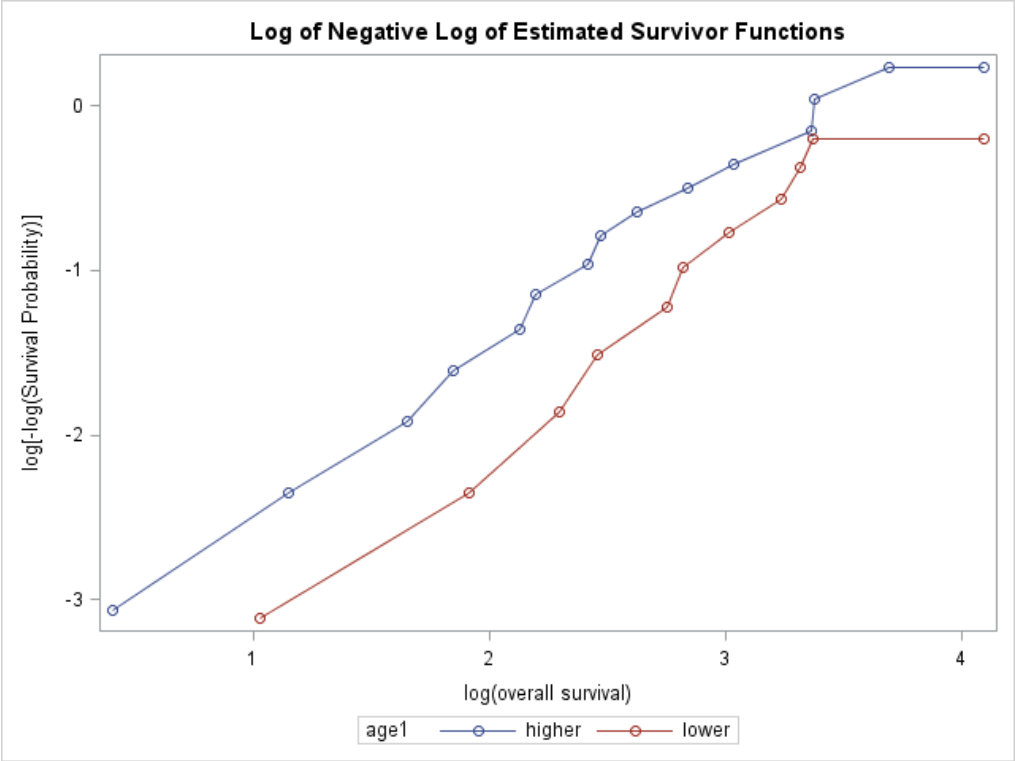
Log of Negative Log of Estimated Survivor Functions
log[-log(Survival Probability)]
0
-1
-2
-3
1
2
3
4
log(overall survival)
age1
higher
lower

8. Sex

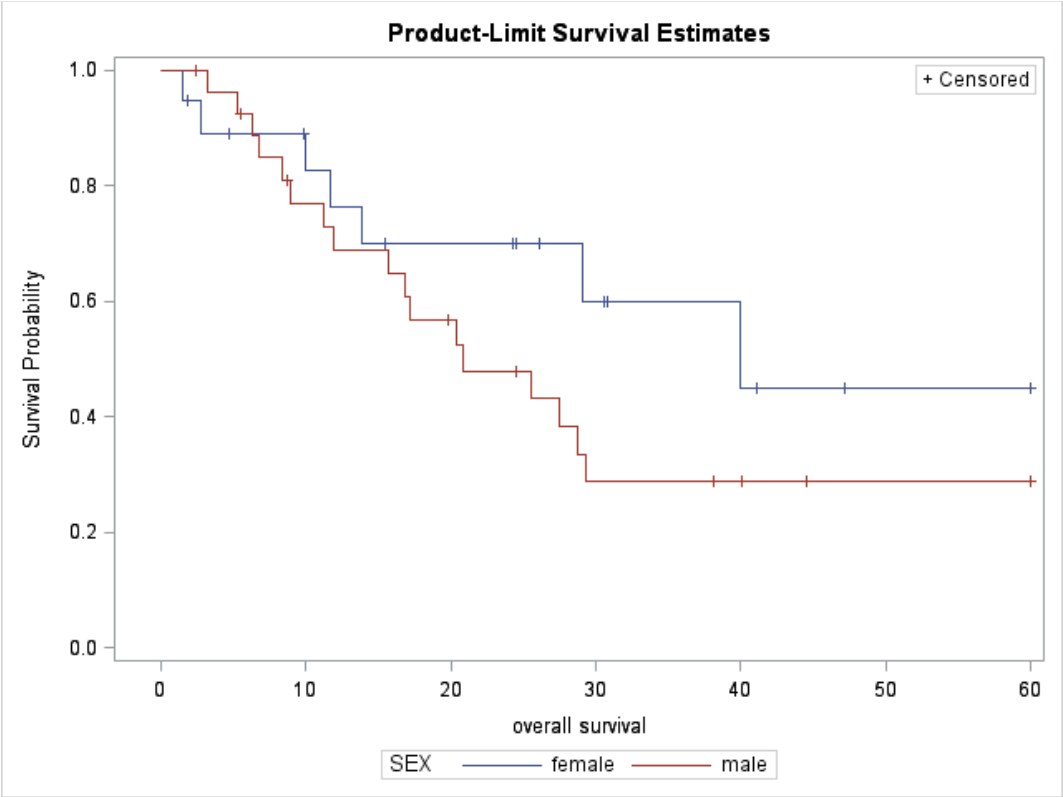
Product-Limit Survival Estimates
+ Censored
Survival Probability
1.0
0.8
0.6
0.4
0.2
0.0
0
10
20
30
40
50
60
overall survival
SEX
female
male

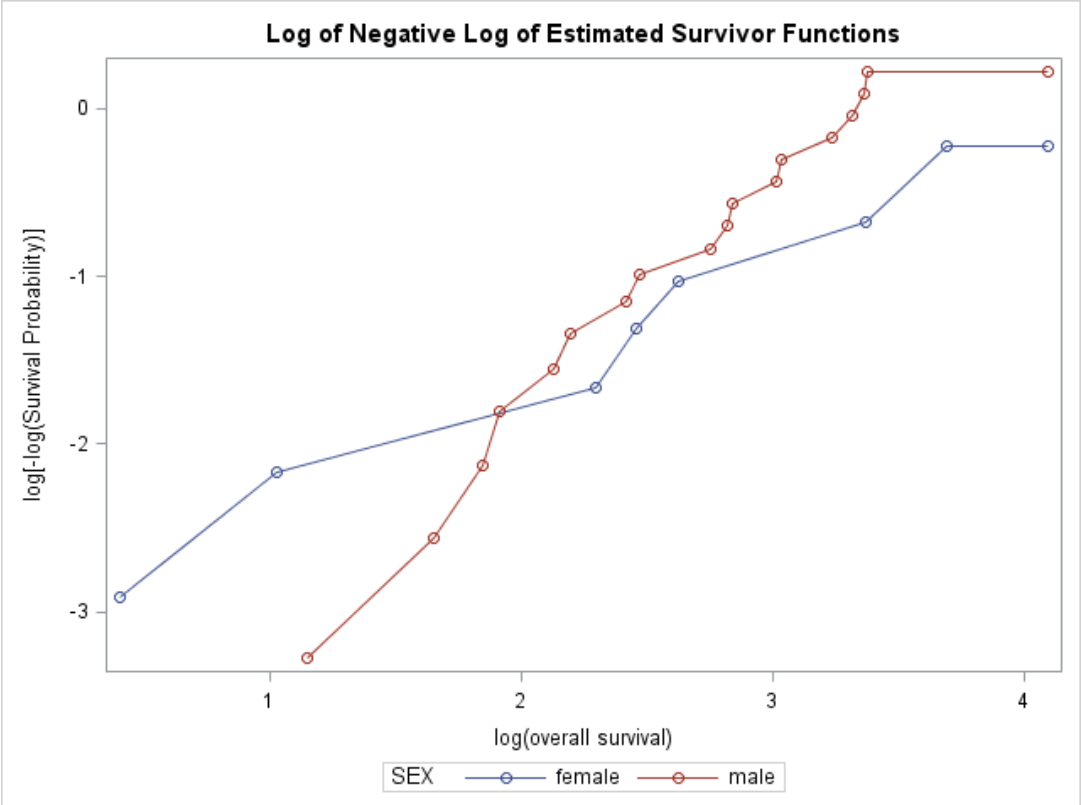
Log of Negative Log of Estimated Survivor Functions
log[-log(Survival Probability)]
0
-1
-2
-3
1
2
3
4
log(overall survival)
SEX
female
male

9. Meld score

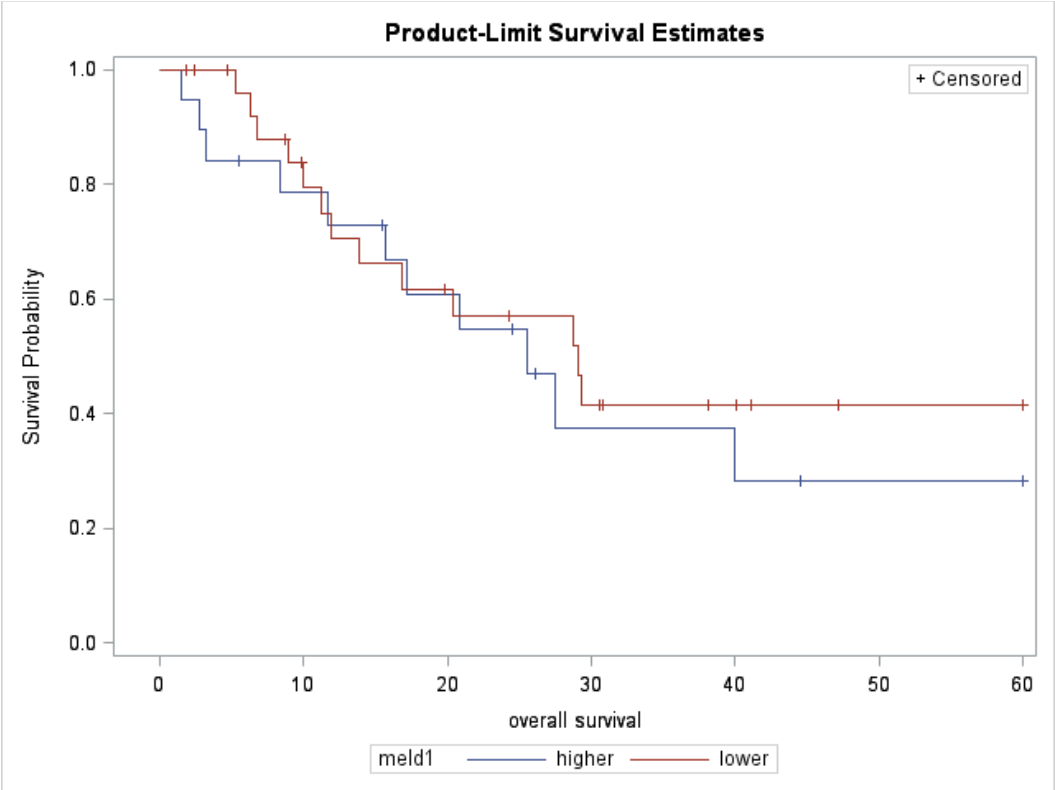
Product-Limit Survival Estimates
+ Censored
Survival Probability
1.0
0.8
0.6
0.4
0.2
0.0
0
10
20
30
40
50
60
overall survival
meld1
higher
lower

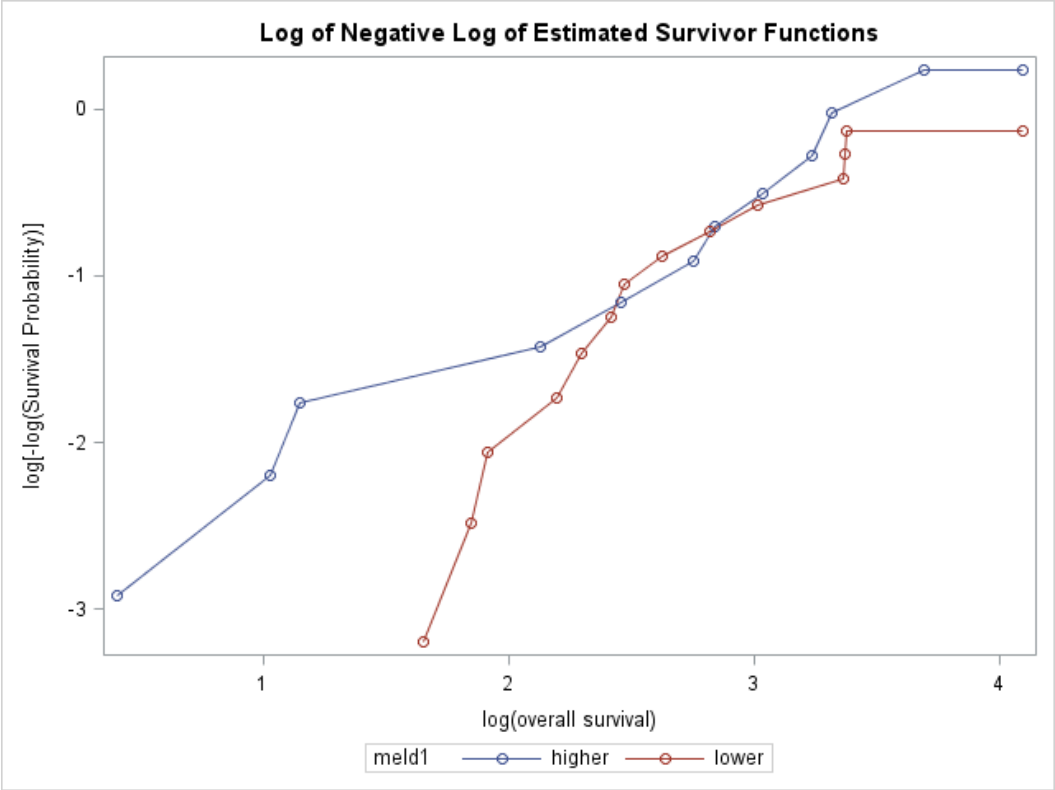
Log of Negative Log of Estimated Survivor Functions
log[-log(Survival Probability)]
0
-1
-2
-3
1
2
3
4
log(overall survival)
meld1
higher
lower

10. Tumor size

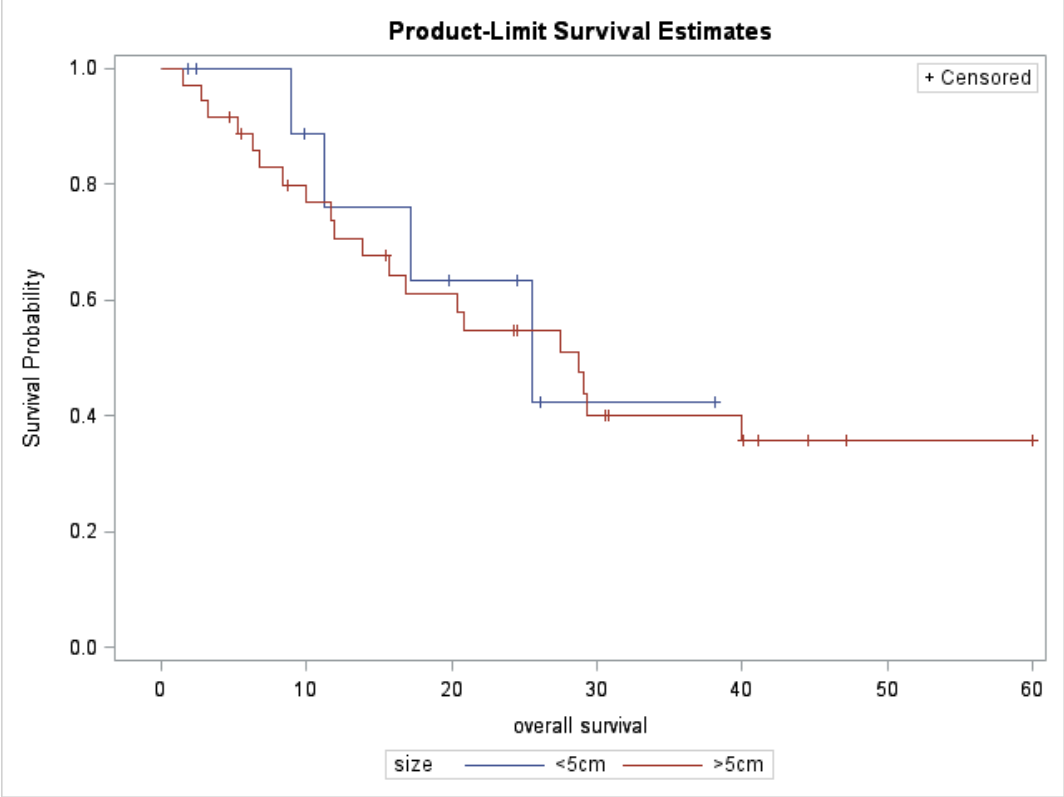

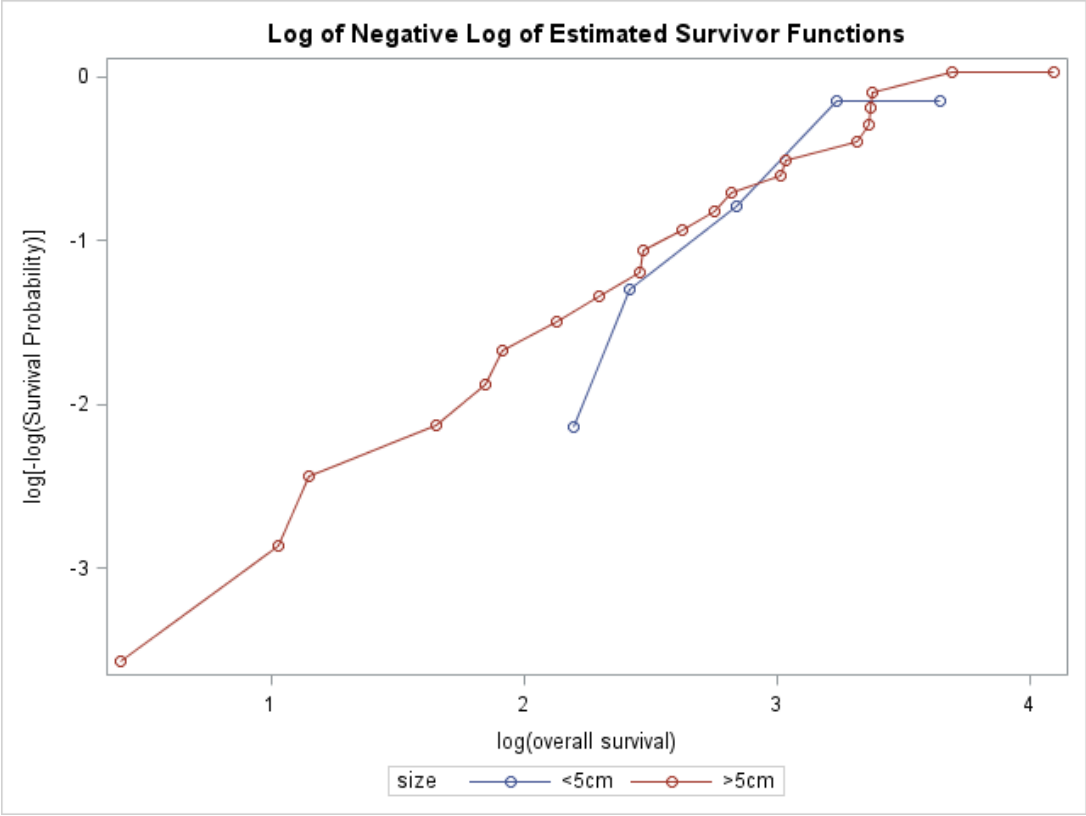

11. Micoscopic margin status

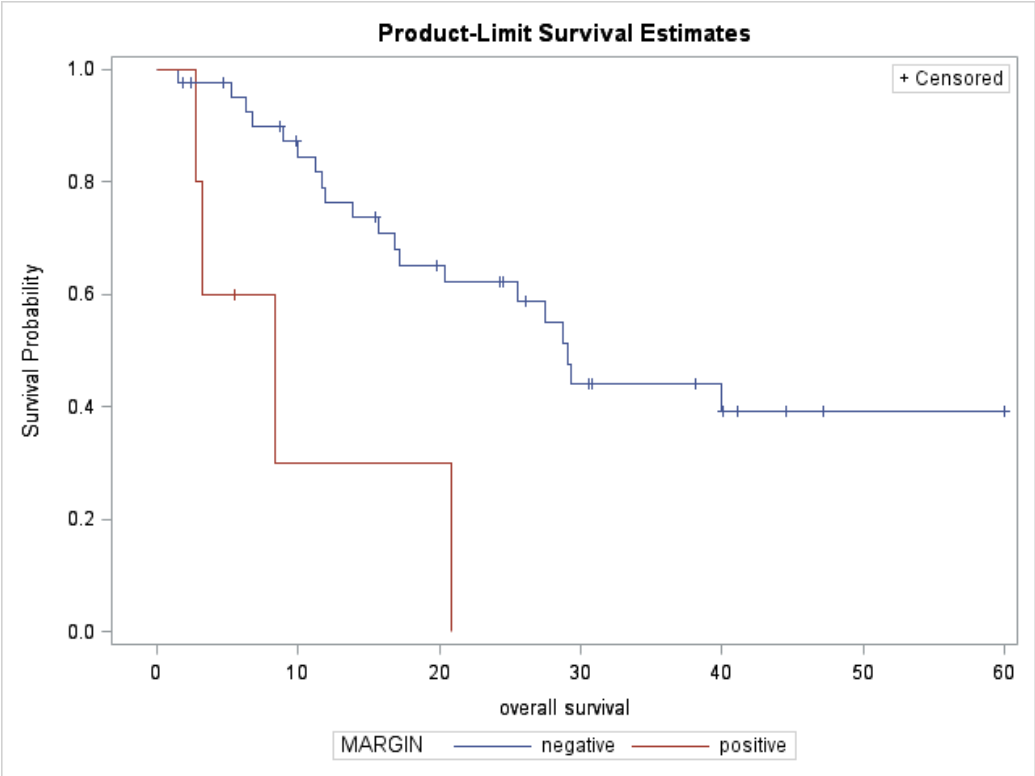

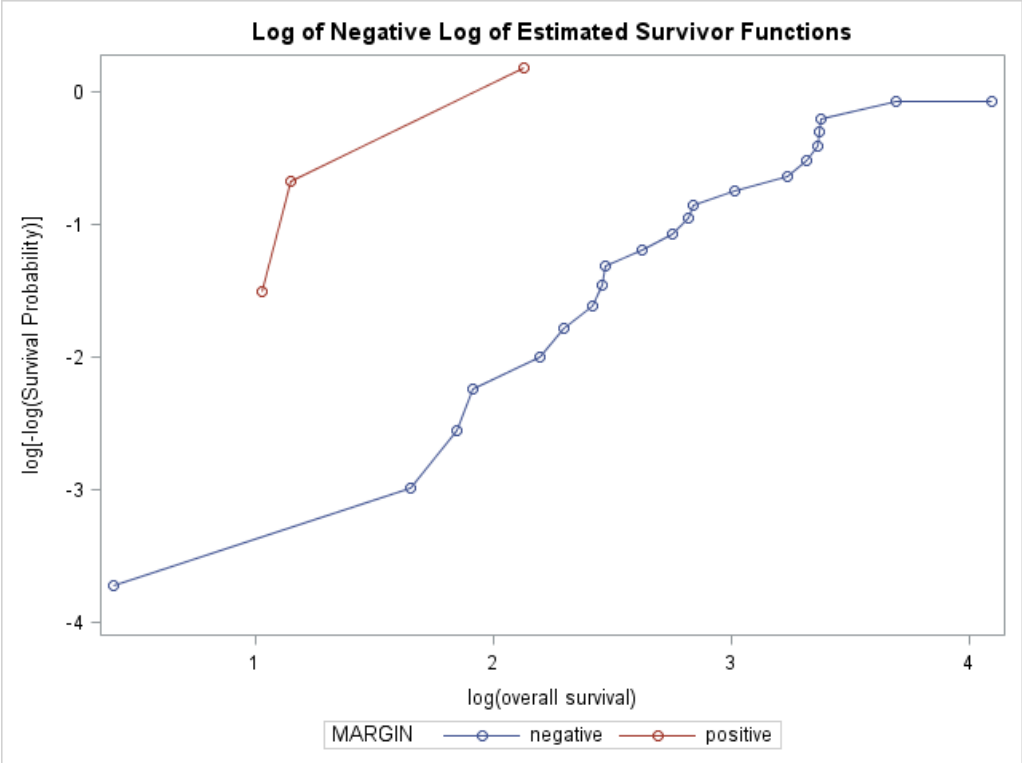

12. Microvascular invasion

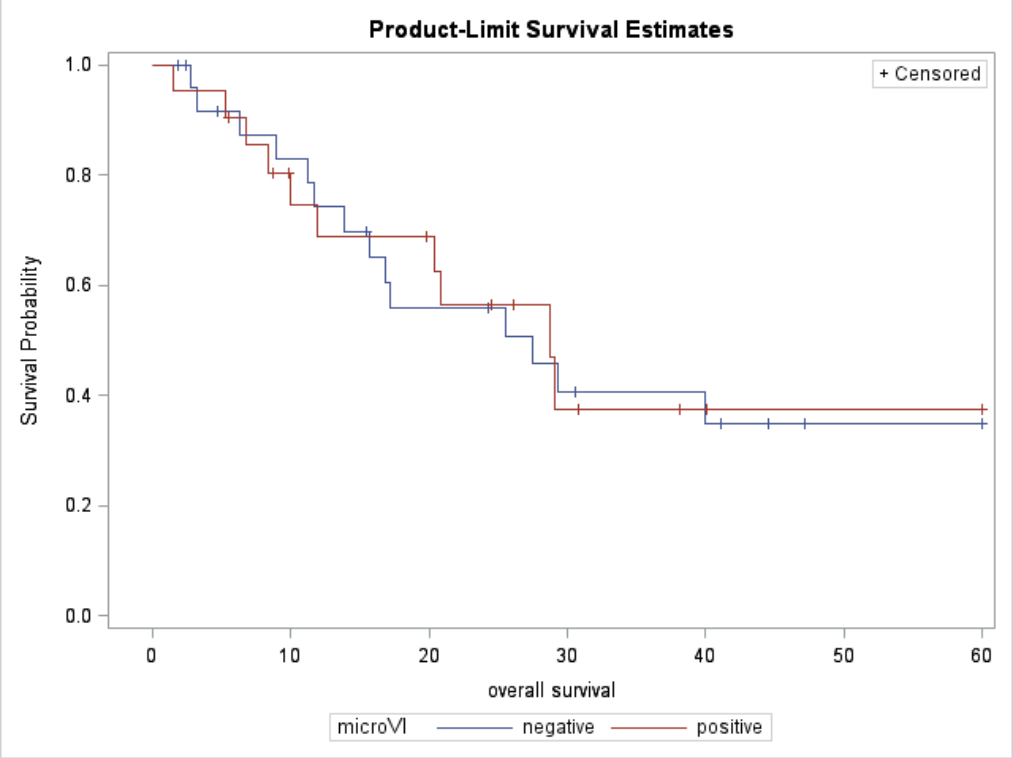

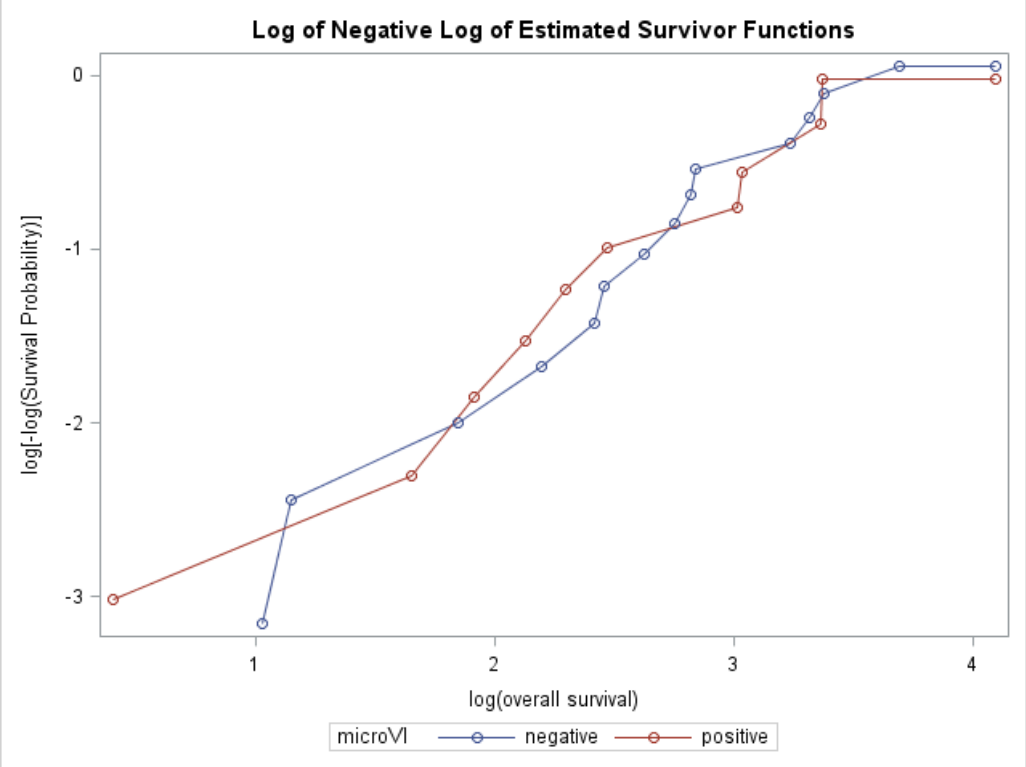

13. PDGFR-α

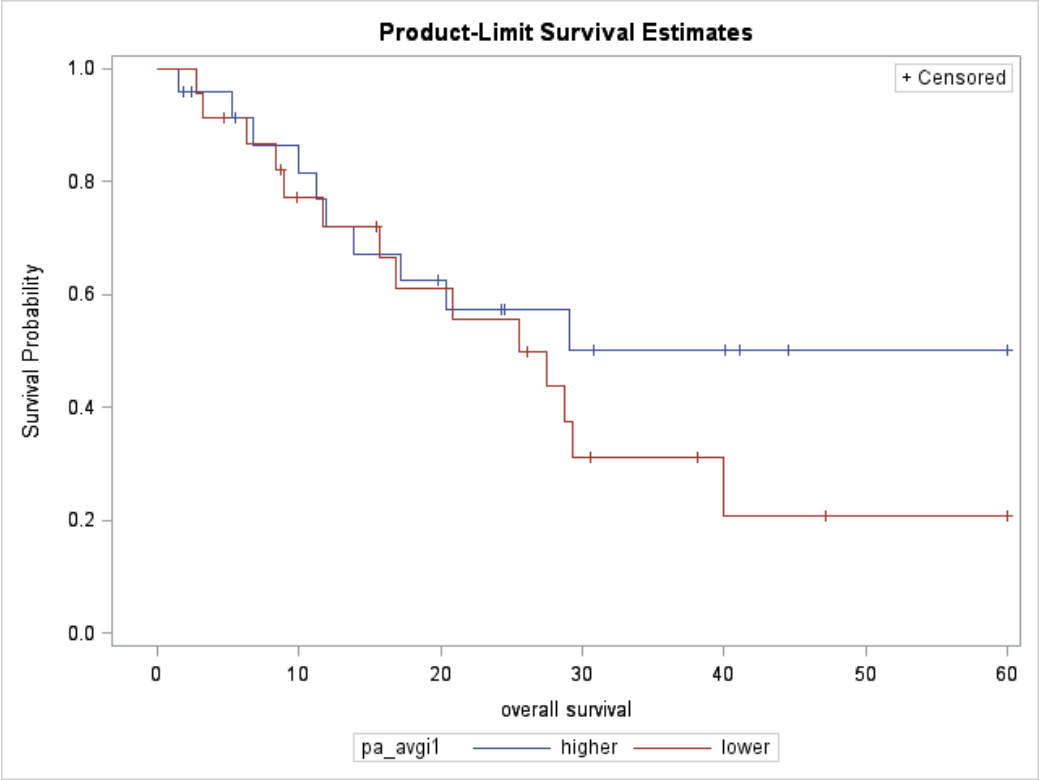
Product-Limit Survival Estimates
+ Censored
Survival Probability
1.0
0.8
0.6
0.4
0.2
0.0
0
10
20
30
40
50
60
overall survival
pa_avgi1
higher
lower

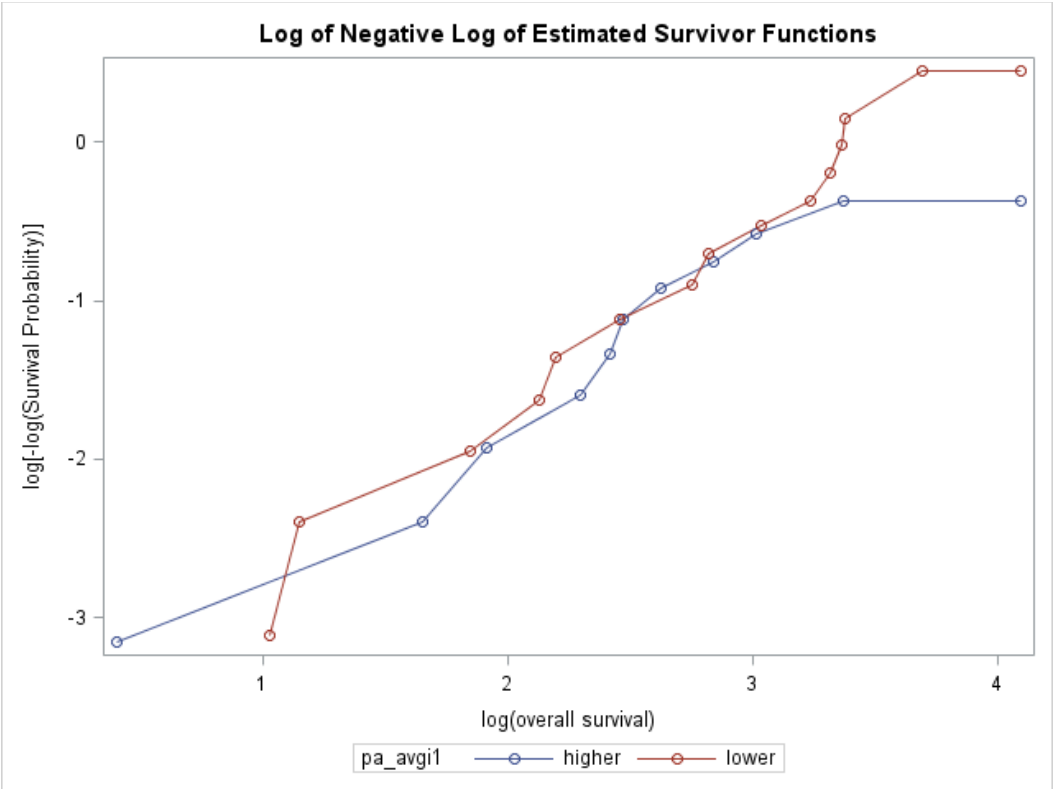
Log of Negative Log of Estimated Survivor Functions
log[-log(Survival Probability)]
0
-1
-2
-3
1
2
3
4
log(overall survival)
pa_avgi1
higher
lower

14. PDGFR-β

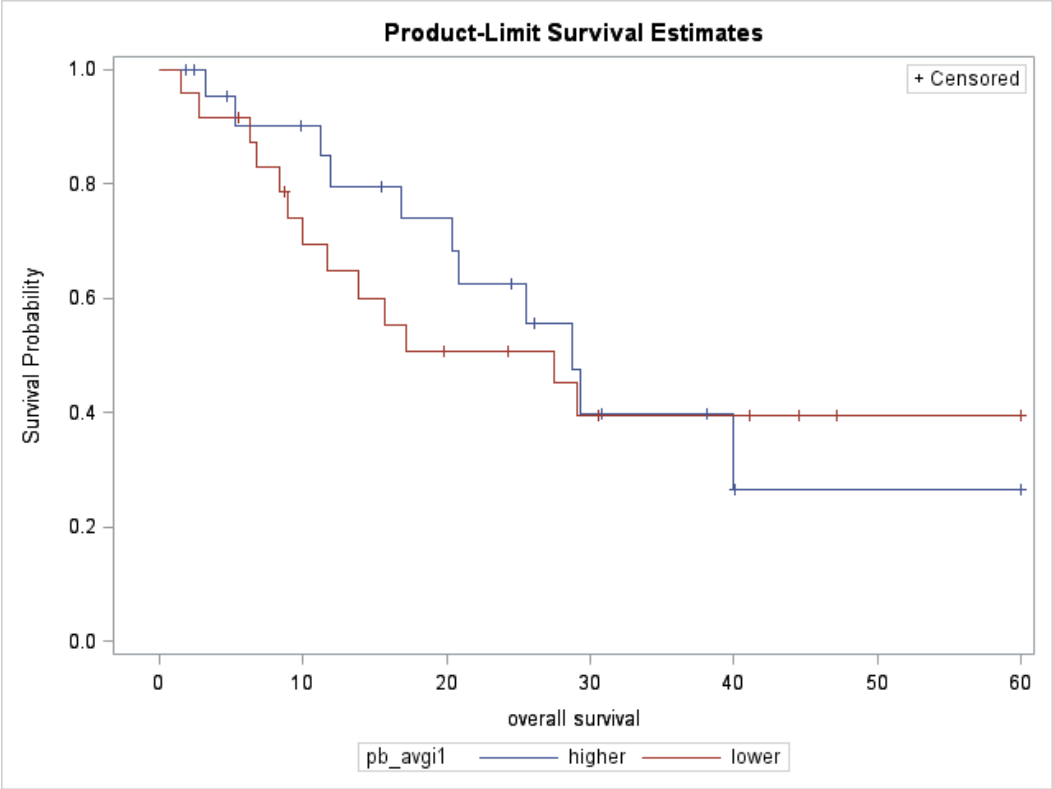
Product-Limit Survival Estimates
+ Censored
Survival Probability
1.0
0.8
0.6
0.4
0.2
0.0
0
10
20
30
40
50
60
overall survival
pb_avgi1
higher
lower

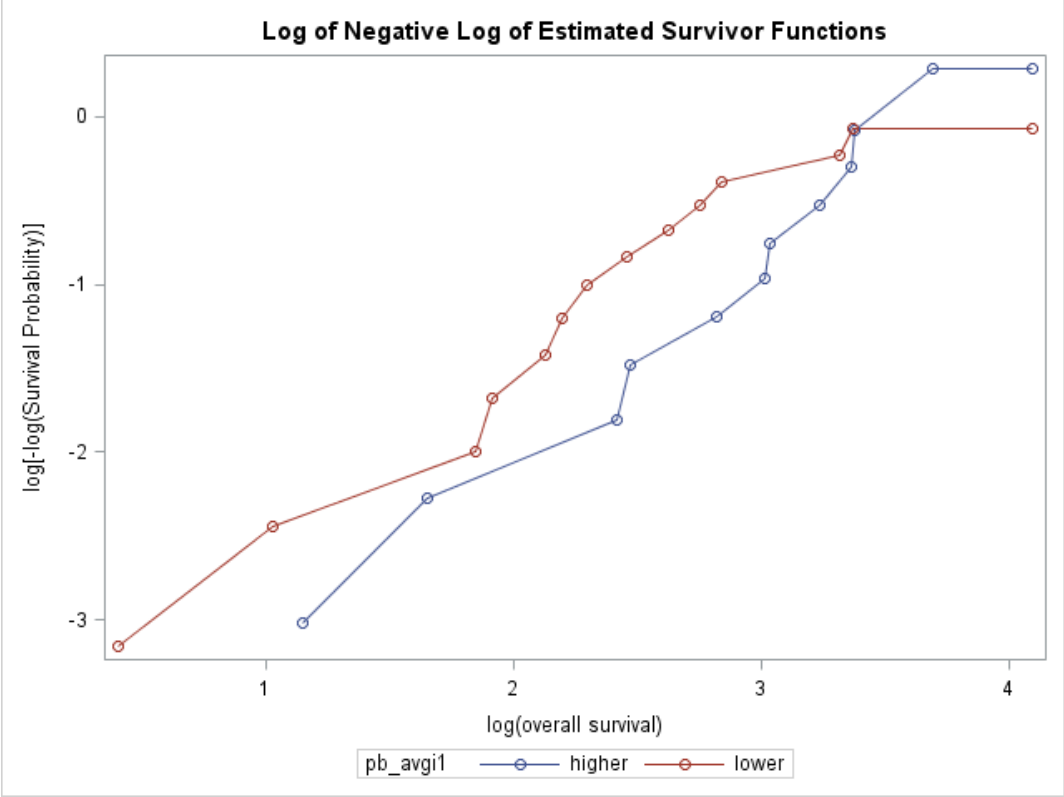
Log of Negative Log of Estimated Survivor Functions
log[-log(Survival Probability)]
0
-1
-2
-3
1
2
3
4
log(overall survival)
pb_avgi1
higher
lower

15. VEGFR2

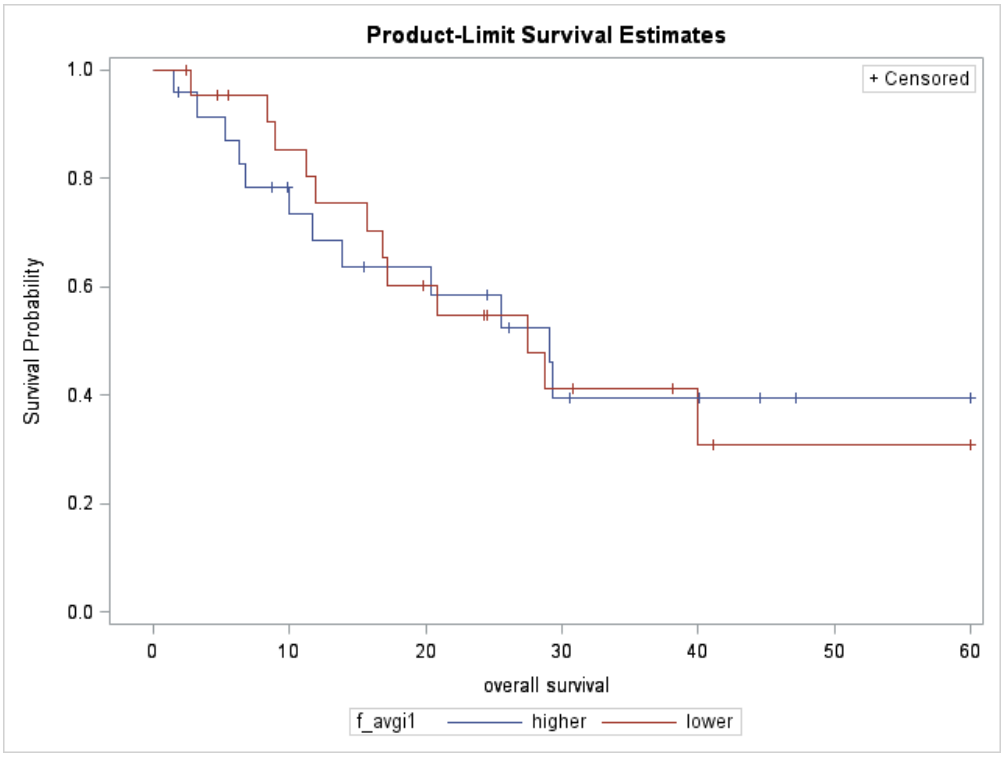
Product-Limit Survival Estimates
+ Censored
Survival Probability
1.0
0.8
0.6
0.4
0.2
0.0
0
10
20
30
40
50
60
overall survival
f_avgi1
higher
lower

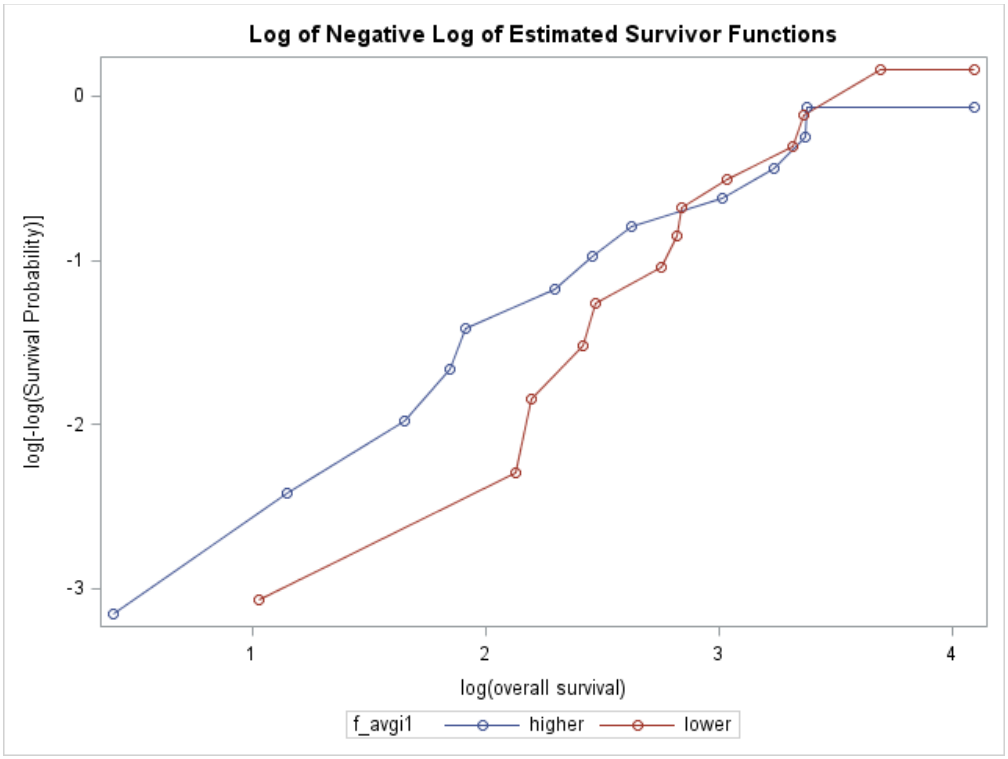
Log of Negative Log of Estimated Survivor Functions
log[-log(Survival Probability)]
0
-1
-2
-3
1
2
3
4
log(overall survival)
f_avgi1
higher
lower